PHYSICAL REVIEW D **80,** 124044 (2009)

Dressing the post-Newtonian two-body problem and classical effective field theory

Barak Kol* and Michael Smolkin†

Racah Institute of Physics, Hebrew University, Jerusalem 91904, Israel

(Received 4 November 2009; published 29 December 2009)

We apply a dressed perturbation theory to better organize and economize the computation of high orders of the 2-body effective action of an inspiralling post-Newtonian (PN) gravitating binary. We use the effective field theory approach with the nonrelativistic field decomposition (NRG fields). For that purpose we develop quite generally the dressing theory of a nonlinear classical field theory coupled to pointlike sources. We introduce dressed charges and propagators, but unlike the quantum theory there are no dressed bulk vertices. The dressed quantities are found to obey recursive integral equations which succinctly encode parts of the diagrammatic expansion, and are the classical version of the Schwinger-Dyson equations. Actually, the classical equations are somewhat stronger since they involve only finitely many quantities, unlike the quantum theory. Classical diagrams are shown to factorize exactly when they contain nonlinear worldline vertices, and we classify all the possible topologies of irreducible diagrams for low loop numbers. We apply the dressing program to our post-Newtonian case of interest. The dressed charges consist of the dressed energy-momentum tensor after a nonrelativistic decomposition, and we compute all dressed charges (in the harmonic gauge) appearing up to 2PN in the 2-body effective action (and more). We determine the irreducible skeleton diagrams up to 3PN and we employ the dressed charges to compute several terms beyond 2PN.

DOI: 10.1103/PhysRevD.80.124044 PACS numbers: 04.25.Nx

I. INTRODUCTION AND SUMMARY

Gravitational wave observatories (see for example the reviews [1] and references therein) demand knowledge of the waveform emitted by an inspiralling binary system of compact objects. Fully generally relativistic (GR) numerical simulations can now simulate such waveforms—see the review [2] and references therein. Yet, as always, an analytic treatment is complementary and improves insight, especially into the functional dependence of the results on the parameters. A *perturbative* analytic treatment is possible in two limits. The first is the post-Newtonian (PN) approximation, and it holds whenever the velocities are small compared with the speed of light, or equivalently through the virial theorem whenever the separation between the compact objects is much larger than their Schwarzschild radii. The second limit is that of an extreme mass ratio. In this paper we shall concentrate on the PN approximation which is always valid at the initial stages of any inspiral.

The computation of the effective 2-body action in PN was a subject of considerable research over the last decades and the current state of the art is its determination up to order 3.5PN, as summarized in the review [3] (see also the recent [4]). Another approach, the effective field theory (EFT) approach to this problem was suggested by Goldberger and Rothstein in 2004 [5], where more traditional GR methods are replaced by field theoretic tools including Feynman diagrams,[1] loops and regularization. In particular [5] reproduced the 1PN effective action (known as Einstein-Infeld-Hoffmann) within the EFT approach. In [7,8] the metric components in the post-Newtonian, nonrelativistic limit were conveniently decomposed into a scalar Newtonian potential, a gravitomagnetic 3-vector potential and a symmetric 3-tensor. These fields were termed collectively ''fields of nonrelativistic gravitation (NRG fields),'' and the derivation of 1PN was shown to further simplify. In [9] the 2PN expression was reproduced within the effective field theory approach together with NRG fields.

Other recent developments related to either PN or the EFT approach include: dissipative effects and effective horizon degrees of freedom [10,11]; thermodynamics of caged black holes [12,13] through the EFT approach [7,14,15]; EFT [16] (see also [17,18]) Hamiltonians [19,20] for rotating point particles; tidal effects for compact objects [21,22]; approximate solutions for higher-dimensional black object including rings [23] and black-folds [24]; a mechanized EFT computation for 2PN [25]; ''De-Turek'' gauge for numerical relativity [26]; and finally radiation reaction and waves within the EFT approach [27,28].

*barak_kol@phys.huji.ac.il
†smolkinm@phys.huji.ac.il

[1]See also [6] for certain early day efforts to calculate classical potentials to higher post-Newtonian orders using field theoretical methods and Feynman graph techniques.

The computation of order 2PN [9] demonstrates a proliferation in the number of diagrams: from 4 at 1PN to 21 at 2PN, and furthermore the number is expected to continue and grow at the next order. Clearly, it would be useful to have an improved perturbative expansion. In this paper we shall present a new method to better organize the calculation and economize it. The basic idea is to recognize recurring subdiagrams which physically describe ''dressed'' charges and propagators. The simplest example is furnished by the Newtonian potential $Gm_1m_2/|r_1 - r_2| \subset S_{\rm eff}$ which belongs to order 0PN. This term is associated with the diagram in Fig. 1. At higher orders there is a class of diagrams of the form shown in Fig. 2 where the point masses are replaced by dressed energy distributions defined on the top row of Fig. 3

$$m_i\delta(x_i - r_i) \rightarrow \rho_{dr}(x_i - r_i) \tag{1.1}$$

and the bare propagator is replaced by the dressed (relativistic) one defined on the bottom of Fig. 3

$$\frac{1}{k^2}\,\delta(\Delta t) \rightarrow G(k, \Delta t). \tag{1.2}$$

The same subdiagrams which define the dressed energy distribution and appear in the calculation of the dressed Newtonian interaction (Fig. 2) appear also in other diagrams. It makes sense to record the values of these subdiagrams and later reuse them. This is the basic idea of the dressed perturbation theory.

In addition, the dressing procedure is shown to economize the calculation in a more significant way as follows. We find that the dressed couplings satisfy a certain recursive integral equation schematically described in Fig. 4. A perturbative expansion of the solution to this equation equals an infinite sum of diagrams, and in this sense it encodes many diagrams. This is nothing but the classical version of the Schwinger-Dyson equations which were first written in the context of quantum electrodynamics [29]. Yet the current classical version is of a higher practical value compared to its quantum counterpart since it does not involve the infinitely many dressed bulk vertices.

Some discussions of classical versions of the Schwinger-Dyson equations appeared already, yet they all appear to consider a significantly different context. Reference [30] studied unequal time correlation functions of a nonequilibrium classical field theory, while [31] aims at giving a construction of the local algebras of observables in quantum gauge theories.

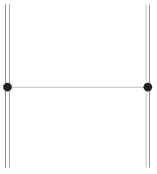

FIG. 1. The diagram which represents the Newtonian-potential interaction mediated through the Newtonian scalar field ϕ. The notations will be fully defined later in Sec. III.

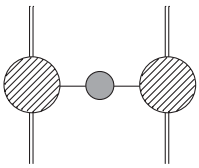

FIG. 2. A class of diagrams that we interpret as the Newtonian-potential interaction between *dressed* energy distributions of each body through a dressed propagator. The dark blobs represent any subdiagram with an arbitrary number of vertices on the worldline and a single external leg for the Newtonian potential. There are no bulk loops, as always in classical physics. The light blob represents any subdiagram with two external legs of the Newtonian potential, which amounts to a propagator with an arbitrary number of retardation insertions.

The paper is divided into two parts. In Sec. II we describe and discuss the dressed perturbation theory for a general classical (effective) field theory, while in Sec. III we apply it to the post-Newtonian theory. We start in Sec. II by considering a simple scalar classical field theory coupled to pointlike particles as the context for introducing the required dressing concepts. In Sec. II A we characterize the fully factorizable diagrams before turning in Sec. II B to our main definition, that of the dressed quantities. In Sec. II C we define the dressed perturbation theory and assert that it is equivalent to the bare theory.

In Sec. II D we explain the recursive integral equation *à la* Schwinger-Dyson and comment on its relation with related concepts. We close the general theory section in Sec. II E with a classification of irreducible skeletons at low loop numbers—diagrams which are neither factorizable nor do they include dressed subdiagrams.

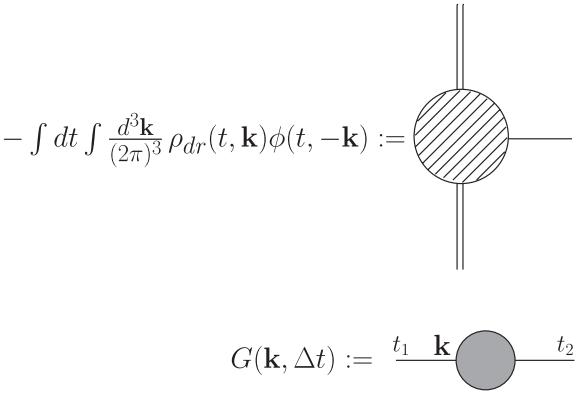

FIG. 3. The diagrammatic definition of the dressed energy distribution (top) and the dressed propagator (bottom). The dressed energy distribution is defined through the one point function for ϕ in the presence of a single source (after stripping external propagators), while the dressed propagator is defined through the full two point function for ϕ.

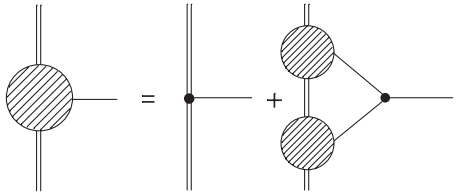

FIG. 4. A schematic diagrammatic representation of the Schwinger-Dyson recursive integral equation satisfied by the dressed couplings. More details are given in the body of the paper.

In Sec. III we apply these concepts of dressing theory to better organize and economize the two-body PN effective action. In Sec. III A we set up the problem by displaying the post-Newtonian effective action and the associated Feynman rules. In Sec. III B we explicitly compute the three charges in PN. The charge which couples to the gravitational field is the energy-momentum tensor, and since the gravitational field naturally decomposes in the PN limit into three NRG fields the source decomposes too into three corresponding parts: the energy density, the momentum density and the stress. These charges are computed both in k space and in position space up to the order required to reproduce the 2PN results, and the stress is determined to one additional order.

In Sec. III C we analyze qualitatively the diagrams relevant to the computation of the two-body effective action. Starting with 0PN and making our way to order 2PN we explain how some of the diagrams can be expressed through dressed charges, and which diagrams can be generated by the integral equation. Up to order 2PN only a single (nontree) diagram is found to be irreducible. We confirmed that the known 2PN effective action is reproduced after incorporating our expressions for the dressed charges from the previous subsection. While thus far almost all the computations are related to the known [3] 2PN effective action which was already reproduced within the EFT approach with NRG fields in [9], here we list all the skeletons required for the computation of 3PN, thereby indicating the road map for organizing the 3PN computation. In Sec. III D we convincingly demonstrate the utility of our method by computing certain novel 3PN and 4PN diagrams.[2] Finally, in the appendix we collect some useful integrals.

II. DRESSED PERTURBATION THEORY IN CLEFT

In this section we define a dressed perturbation theory in the general classical effective field theory (CLEFT) context, namely for any classical nonlinear field theory coupled to pointlike sources.

In order to illustrate the main ideas in a simple setting we consider a scalar field model. The generalization to an arbitrary CLEFT is straightforward and will be spelled out at the end of Sec. II B.

Consider the following bulk action

$$S_{\rm bulk}[\phi] = \int d^4x \left[-\frac{1}{2}(\vec{\nabla}\phi)^2 + \frac{1}{2c^2}\dot{\phi}^2 - \frac{\alpha}{6}\phi^3 \right] \quad (2.1)$$

for a scalar field ϕ with propagation speed c and coefficient of cubic interaction α, where ϕ couples to any point particle of mass m and charge q through

$$S_p = -(m-q)\int d\tau - q\int e^{\phi(x(\tau))}d\tau, \quad (2.2)$$

$d\tau$ is the proper time element and the particles will be assumed nonrelativistic $d\vec{x}/d\tau \ll c$ (or even static in part of the discussion). *The total action* for a many body system is

$$S = S_{\rm bulk} + \sum_a S_{p,a}, \quad (2.3)$$

where $S_{p,a}$ is the worldline action (2.2) of the ath particle characterized by m_a, q_a.

Let us briefly discuss the considerations for choosing this form of the action. The retardation term proportional to $1/c^2$ is considered as a small perturbation in the nonrelativistic limit and represents a general small perturbation of the quadratic term. The term proportional to α was chosen to represent any nonlinear interaction. The interaction term $-q\int \exp(\phi(x(\tau)))$ includes the charge coupling $-q\int \phi(x(\tau))$ together with some representative nonlinear terms (this exponential form of the interaction appears in post-Newtonian theory, for example).

The bulk theory (2.1) has a vacuum at $\phi = 0$ and we consider the perturbation theory around it. As usual, we note that while this vacuum is unstable, it could be stabilized by adding a mass term to $S_{\rm bulk}$, and it could even be made a global minimum through the addition of a quartic term in the potential.

In this paper we study the *two-body problem* rather than the seemingly more general *many body problem* since it is the simplest and currently the most interesting case. The generalization to the many body problem seems straightforward.

The *Feynman rules* involving ϕ are shown in Fig. 5. They are standard except for the CLEFT conventions which makes them real—vertices are read from the action and propagators are given schematically by $-1/S_2$ where S_2 is the quadratic part of the action. See [7] for the original definition and full detail.

The two-body effective action is defined by

$$S_{\rm eff}[x_1, x_2] := S[x_1, x_2, \phi(x_1, x_2)] \quad (2.4)$$

[2]The computed first post-Minkowskian approximation [32] includes information about a certain class of diagrams to arbitrarily high PN orders, which are different however from the ones we compute here.

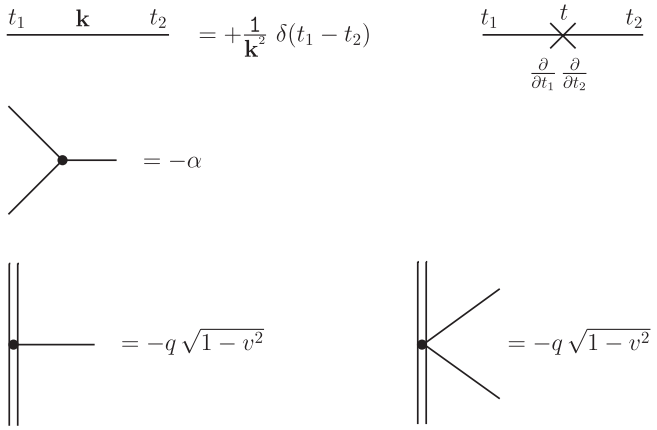

FIG. 5. The Feynman rules involving ϕ for the static scalar field theory whose action is given by (2.3). The rules describe: the propagator and the quadratic perturbation vertex—retardation (top), the cubic bulk vertex (middle), and the worldline vertices (bottom) where the ellipsis stands for additional nonlinear worldline vertices. Hereafter k denotes a spatial wave number.

where the right-hand side (rhs) represents the action (2.3) evaluated on the solution $\phi = \phi(x_1, x_2)$ given the particle trajectories $x_1(\tau_1), x_2(\tau_2)$. The effective action is known to be equal to the sum of all connected Feynman diagrams made out of ϕ propagators with arbitrary bulk vertices and worldline vertices but without loops of propagating fields (such classically forbidden loops are allowed quantum mechanically).

A. Factorizable diagrams

There are several possible paths to classical dressed perturbation theory. We shall build it from first principles and later discuss its relations with both the quantum version and the standard classical theory.

The main idea is to economize the perturbation theory by identifying certain recurring subdiagrams. Before we proceed to the more essential, dressed subdiagrams we discuss a stronger and simpler form of reduction, namely factorizable diagrams.

A Feynman diagram is called *factorizable* whenever the expression which it represents factorizes (into a product of factors), each one corresponding to a subdiagram. An example is shown in Fig. 6. In CLEFT we have the interesting property that *a diagram of the 2-body effective action is factorizable if and only if it contains a nonlinear worldline (NL-WL) vertex*, where a NL-WL vertex is a vertex with more than a single bulk field.

Indeed, if a diagram contains a NL-WL vertex then since quantum loops are not allowed, each leg of the vertex generates a separate subdiagram. Conversely, a connected[3] factorizable diagram necessarily factorizes at a vertex. A bulk vertex would not serve since wave number conservation couples between all its legs.[4]

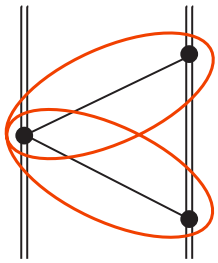

FIG. 6 (color online). An example of a factorizable diagram (the simplest). The two factors are circled (in red) and they intersect in a NL-WL vertex. A diagram of this type appears at 1PN—see Fig. 23.

B. Dressed charge and propagator

Following our discussion of factorization we proceed to consider only diagrams without any NL-WL vertices. Any nonfactorizable diagram contains various subdiagrams. We wish to further economize the perturbation theory by identifying in a unique and natural way a class of subdiagrams which repeatedly show up at high orders of the two-body effective action. We shall call them "dressed subdiagrams." We start with constructive definitions and an explanation of the name's origin, to be followed by a more abstract characterization through an equivalence of perturbation theories which serves to explain the rationale behind the definitions.

Definitions

(i) The *dressed charge of the particle*, $\rho_{dr}(k, t)$ is defined diagrammatically through Fig. 7 (top). The dressed charge is an infinite sum of subdiagrams, where each summand will be called a *dressed charge subdiagram*.

(ii) The *dressed propagator*, $G_{dr}(k, \Delta t)$ is defined diagrammatically through Fig. 7 (bottom). Each summand in the definition will be called a *dressed propagator subdiagram*.

Let us inspect these definitions. In equations $\rho_{dr}(r)$ is defined through

$$\rho_{dr}(r, t) := \triangle\Phi(r, t) = \int d\tau q\delta^{(4)}(x - x(\tau)) + \frac{1}{2}\alpha\Phi^2 + \partial_i^2\Phi \quad (2.5)$$

where the second equality is a differential equation which together with retarded boundary conditions defines $\Phi(r, t)$,

[3]All the diagrams of the 2-body action are connected by definition.

[4]In CLEFT we cannot have a factorizable diagram such as the "figure 8" diagram in ϕ^4 theory, since we cannot have k conservation for any strict subset of propagators leaving the bulk vertex, as each propagator connects to a distinct worldline vertex (or vertices) where k is arbitrary.

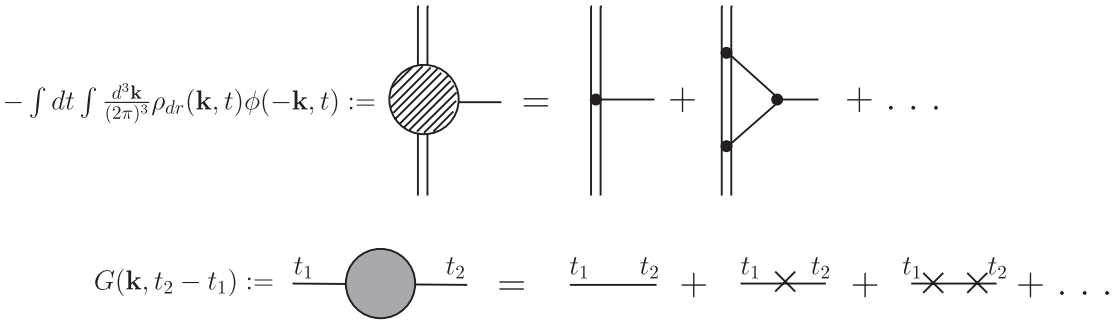

FIG. 7. The diagrammatic definition of the dressed charge distribution (top) as the one point function for ϕ in the presence of a single source and the dressed propagator (bottom) as the full two point function for ϕ in vacuum. Retardation vertices are forbidden on the external leg of the dressed charge.

the full solution for the field ϕ in presence of the given source worldline. This equation is equivalent to the diagrammatic definition since Φ is given diagrammatically by Fig. 8, and hence in k space $\Phi(k, t) = -\rho_{dr}(k, t)/k^2$ from which (2.5) follows in position space.

The dressed charge describes the apparent particle charge (distribution) at long distances. It arises from the nonlinear interactions of the scalar field which "dress" the point charge, and is useful for studying the dynamics of a system composed of several such particles. The term which we use, "dressed" charge (and propagator) is standard terminology in quantum field theory (QFT) (see for example [33]) as well as in classical field theory. For completeness we would like to mention some related terms. The first is renormalization, where like here one replaces a bare quantity by a scale-dependent renormalized quantity which is defined through the divergences of the same subdiagrams.[5] Another related term is resummation where one discusses partial sums of diagrams.

The equation form of the dressed propagator is

$$G_{dr} = \frac{1}{\Box} = \frac{1}{k^2 + \partial_t^2/c^2} = \frac{1}{k^2}\frac{1}{1 + \partial_t^2/(c^2k^2)} = \frac{1}{k^2}\left(1 - \frac{1}{c^2k^2}\partial_t^2 + \frac{1}{c^4k^4}\partial_t^4 + \cdots\right) \tag{2.6}$$

where the last equality is a representation of the series on the left of Fig. 7 (bottom), while the previous expressions can be considered to be a closed form summation of that series.

[5]The idea of renormalization in the PN context appeared already in the literature. Reference [34] associated renormalization with the regularization of certain divergences which appear in the particle's effective action at order 3PN. Reference [5] studied the same divergences from the EFT approach and in particular they computed the renormalization of the energy-momentum tensor of a static particle up to 2 loops. Later [35] also studied the renormalization of the energy-momentum tensor.

Physically, in this field theory and also in PN the dressed propagator is nothing but the fully relativistic propagator. However, this need not be the case in general.

Example. To illustrate these ideas let us discuss an example. A detailed application to the post-Newtonian theory will be given in Sec. III.

Consider the 6-loop Feynman diagram in Fig. 9(a) which contributes in the bare theory to the 2-body effective action. It has five dressed subdiagrams (circled)—two dressed charges and three dressed propagators. Note that all the worldline vertices of each dressed charge belong to *one and the same* point particle. Note also that retardation vertices are allowed inside the dressed charge but not on its

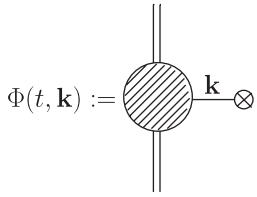

FIG. 8. The diagrammatic representation for the value of the field in the presence of the point-particle source. The only difference with the definition of the dressed charge in Fig. 7 (top) is an added propagator on the external leg.

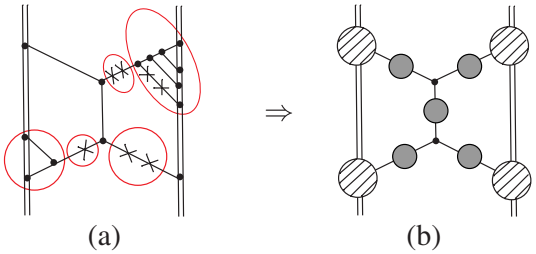

FIG. 9 (color online). An example for the correspondence between diagrams of the bare theory, such as (a) and the corresponding dressed diagram (b). Note a standard subtlety: retardation insertions are allowed inside a dressed charge vertex, but not on its external leg. See text for further discussion.

external leg. Upon replacing the dressed subdiagrams by dressed vertices and propagators we obtain the diagram's skeleton[6] in 9(b). The resulting diagram is only two-loop. The other loops were absorbed by the dressed charges. Note that the 3-loop dressed charge subdiagram includes in it other dressed subdiagrams, but these are not maximal.

Generalization. So far we worked in a simple setting of a cubic scalar field model. Here we shall indicate how the definitions given above for the dressed subdiagrams generalize to a general field theory.

In the scalar field theory we had a single dressed vertex and a single dressed propagator. In a general classical field theory interacting with pointlike particles we have a dressed charge for each field. For the dressed charge to be nontrivial the bulk theory must be interacting.

The dressed propagator in a general field theory is labeled by any two fields that can "mix." In case the fields do not mix then we have a single dressed propagator for each field. For the dressed propagator to be nontrivial we need the quadratic Lagrangian to decompose into a leading part and a perturbation, so that the leading part will determine the bare propagator, while the small part will determine the two-vertex. The dressed propagator will then be proportional to the inverse of the full quadratic Lagrangian. We note that one may choose to diagonalize the dressed propagator and accordingly redefine the fields such that there will be no mixing through dressed propagators.

C. Equivalence of perturbation theories

We proceed to define a dressed perturbation theory, which is equivalent to the original one, but somewhat more economic.

Definition. A Feynman diagram which includes a nontrivial dressed subdiagram of the form shown in Fig. 7 (*dressing subdiagram*) will be called *dressing-reducible*. Otherwise it will be called *dressing-irreducible*.

Definition. The *dressed perturbation theory* is defined as follows

(i) Figure 10 shows the changes in Feynman rules relative to the original theory (Fig. 5).
(ii) Only dressing-irreducible diagrams are allowed.

The original perturbation theory will be distinguished from the dressed one by referring to it as *bare*.

Property—The bare and dressed perturbation theories are equivalent: each diagram of the bare theory is included exactly once in a dressed diagram.

This property is analogous to a standard one holding for dressed actions in QFT, and we shall outline a proof. Given a bare diagram we claim that its maximal dressed subdiagrams are unique. We find the uniqueness property to be quite apparent when one thinks about it, but we shall not attempt to provide a proof here, as it seems tedious. Given

[6]This term will be further discussed and defined in the next subsection.

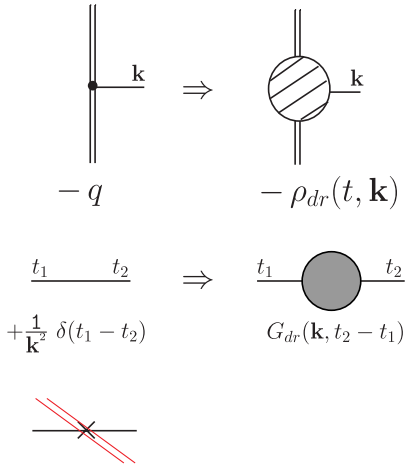

FIG. 10 (color online). The dressed Feynman rules contain changes relative to the bare Feynman rules in Fig. 5. The bare worldline vertex (charge) Feynman rule changes into the dressed one, the bare propagator changes into the dressed one, and the retardation rule is omitted. The rest of the rules remain unchanged.

the decomposition we replace the dressed subdiagrams by propagators and vertices of the dressed theory according to Fig. 10. The resulting reduced diagram is called *the skeleton* of the original diagram. The uniqueness of decomposition implies now that each bare diagram is included once and only once in the dressed perturbation theory, and hence the two are equivalent.

Discussion. Before proceeding to describe another property of the dressed theory, namely, the integral equation, let us pause to discuss some aspects of the definitions and property above.

Rationale behind definitions. The decomposition into a skeleton with blobs which represent dressed subdiagrams is natural in a practical, computational sense. When computing a diagram, the dressed subdiagrams are almost inevitably evaluated on the way, by their nature. Hence it is computationally natural to prepare a list of dressed subdiagrams and their value, in order to avoid their repeated evaluation, which is exactly what the dressed theory does.

Yet, the computational argument alone does not fix our definitions of the dressed subdiagram. *The characterizing property is precisely the equivalence property above*, namely that the dressed perturbation theory is equivalent to the bare one, or in other words, *the dressed theory is self-sufficient or autonomous*. We claim (again without proof) that this property can be used to *derive* our definitions.

Analogy with effective action in QFT. The ideas above are analogous to those of the effective action in standard QFT. There one collects all the 1-particle-irreducible (1PI) diagrams into the effective action and then allows in the perturbative expansion only tree diagrams of the effective action. In both cases it is important that the decomposition

is unique—any diagram can be uniquely divided into 1PI subdiagrams which allow a reduction to a tree skeleton.

Relation of the dressed subdiagrams with the "dressed source" in standard QFT. The two notions are essentially the same. Note however that unlike some cases, for us it is important that the dressed charge subdiagrams are only those where all worldline vertices belong to one and the same point particle.

Our notion of the dressed propagator is also essentially the same as the dressed propagator and the associated field strength renormalization in standard QFT. The 2-vertex in CLEFT is the "self-energy" (the 1PI two point function), and (2.6) is essentially the standard QFT relation between the self-energy and the dressed propagator. The difference is that in QFT many diagrams can contribute to the self-energy (actually normally they are infinitely many corresponding to an arbitrary number of possible loops) while in CLEFT the 2-point vertex is read directly from the Lagrangian.

Why is the dressed propagator necessary? Consider doing away with the definition of the dressed propagator by allowing the dressed vertex subdiagrams to include retardation vertices on the external leg. In the classical theory this would actually work in all but one important class of diagrams, that of the dressed Newtonian interaction—Fig. 2, where the correspondence between the bare and dressed diagrams would break. For example, consider the diagram in Fig. 11. There are two distinct ways to cut the diagram into subdiagrams, the cuts being denoted by (a) and (b). Accordingly this diagram is doubly counted in the putative dressed theory, thereby disqualifying it. This is all the better since the dressed propagator is an appealing physical concept which we would not want to lose anyway.

D. Schwinger-Dyson recursive integral equation in CLEFT

In this section we shall describe a second property of the dressed perturbation theory: certain recursive relations which generally take the form of integral equations. We start by considering the static limit of the scalar theory (2.3) where the idea is simpler to illustrate and later we refine it to include the general nonstatic case.

Recall the definition of $\rho_{dr}(r)$ in Fig. 7.

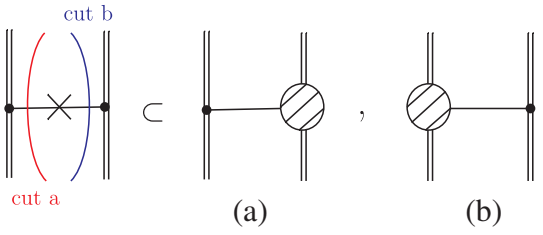

FIG. 11 (color online). An overcounting problem with an alternative definition of the (nonstatic) dressed perturbation theory, as discussed in the text.

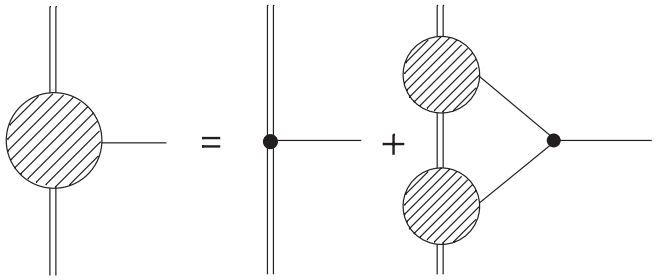

FIG. 12. The diagrammatic representation of the recursive integral equation satisfied by the dressed charge in the static limit.

Property. The dressed quantities satisfy recursive relations. In the static limit $\rho_{dr}(r)$ satisfies the recursive relation which is shown diagrammatically in Fig. 12. Its equation form reads

$$-\int \frac{d^3k}{(2\pi)^3}\rho_{dr}(k)\phi(-k) = -q\phi|_{\vec{r}=0} - \frac{\alpha}{2}\int \frac{d^3k}{(2\pi)^3}\int \frac{d^3k_1}{(2\pi)^3} \times \frac{\rho_{dr}(k_1)}{k_1^2}\frac{\rho_{dr}(k-k_1)}{(k-k_1)^2}\phi(-k). \tag{2.7}$$

After factoring out $\int d^3k\phi(-k)/(2\pi)^3$ we are left with the following integral equation for $\rho_{dr}(k)$

$$\rho_{dr}(k) = q + \frac{\alpha}{2}\int \frac{d^3k_1}{(2\pi)^3}\frac{\rho_{dr}(k_1)}{k_1^2}\frac{\rho_{dr}(k-k_1)}{(k-k_1)^2}. \tag{2.8}$$

Given a small α the integral equation can be solved perturbatively in α by expanding $\rho_{dr}(k) = \sum \alpha^n \rho^{(n)}(k)$. The zeroth order is given by $\rho^{(0)}(k) = q$, the first order is given by $\rho^{(1)}(k) = \frac{1}{2}\int d^3k_1/(2\pi)^3 \alpha \frac{q}{k_1^2}\frac{q}{(k-k_1)^2}$ and so on. This iterative solution of the integral equation is precisely equivalent to the diagrammatic expansion in Fig. 7 [because they both compute the same quantities, namely $\rho^{(n)}(k)$].

The advantage of the integral equation over the diagrammatic expansion is that it is shorter and economizes the computation by avoiding the need to identify all the necessary diagrams and compute them. Some readers may benefit from the following analogy: the relation between the recursive relation and the full diagrammatic expansion is analogous to the relation between defining a function through a differential equation and defining it through the corresponding power series which solves the differential equation.

The nonstatic case. Once we restore time dependence into the action (2.3) we expect the dressed propagator to have a role in the recursive relations as well. First, it has a recursive relation of its own given diagrammatically by Fig. 13 (bottom). In this case the recursive relation is actually algebraic rather than integral, and hence the closed form solution (2.6) exists. Secondly, the recursive relation for the dressed vertex (Fig. 12) is refined to include the dressed propagator and is now given by Fig. 13 (top).

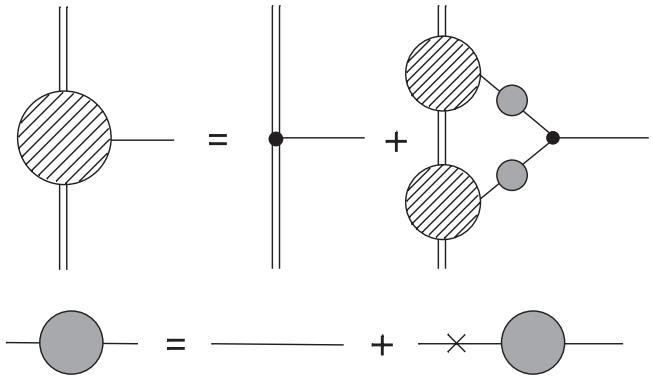

FIG. 13. A diagrammatic representation of the full set of (the two) recursive equations satisfied by the dressed charge (top) and propagator (bottom) in the general, nonstatic case. Note a change in the recursive relation for the dressed charge relative to the static equation in Fig. 12.

We now proceed to make several comments.

(i) The recursive relation [Figs. 12 and 13 and Eq. (2.8)] can be considered as inherited from its quantum version (see for example [36]), but there are interesting differences. As it is, Fig. 12 does not hold in *quantum* field theory[7] because there can be additional ϕ propagators connecting the two blobs on the rhs. Since such additional propagators would create a closed loop of propagating fields it is forbidden in CLEFT. In order for the recursive integral relations to apply in the quantum case one must generalize them to include the dressed bulk vertices yielding the celebrated Schwinger-Dyson equations [29]. However, as stated in several textbooks the practical usefulness of the quantum version is rather limited since more and more Green's functions with more external legs participate in the equations as the order is increased[8] while in CLEFT the equations are more practical exactly because there are only a finite number of dressed quantities.

(ii) The dressed mass $\rho_{dr}(r)$ is closely related to the field profile $\Phi(r)$ generated by the pointlike source. Indeed, each one of them is sufficient to determine the other through (2.5). While $\rho_{dr}(r)$ satisfies an integral equation, $\Phi(r)$ satisfies a "mirror" differential equation, namely the equation of motion given by the second equality in (2.5). The perturbative expansion of the integral equation is dual in turn to the perturbative expansion of the differential equation into some sort of a power series (which will generally include log factors as well).

(iii) Relation with the beta function. The recursive integral equation [(2.8), and Figs. 12 and 13] determines $\rho_{dr}(k)$ and so does the beta function. Yet, the two equations are different as the beta function is a first order differential equation for $d\rho_{dr}/d\log(k)$. Therefore it must be that the beta function equation is a special or limiting case (whose precise definition will not be pursued here) when the leading behavior of ρ_{dr} is logarithmic in k.

E. Irreducible 2-body skeletons

Consider the nonlinear worldline vertices (NL-WL vertices) in the scalar action (2.3), namely vertices with more than a single bulk field. Our definition of the dressed charge concerns a worldline vertex with a single bulk field. It is possible to generalize the definition of the dressed vertex to any number of bulk fields, such as the 2-field vertex shown on the top line of Fig. 14. In this way one may define a *fully dressed one body effective action*.

However, for the purpose of computing the 2-body effective action *we use only the dressed charges (and propagators) and for the NL-WL vertices we use the bare vertices rather than the dressed ones* because they would have created a problem: the decomposition of diagrams would not have remained unique (just as in our discussion around Fig. 11). For example, the diagram on the second row of Fig. 14 can be decomposed in two *different* ways by the two shown cuts, and that corresponds to doubly counting this diagram in the putative fully dressed perturbation theory.

Recall (Sec. II A) that nonlinear worldline vertices are interesting for another, complementary property: *a diagram of the 2-body effective action is factorizable if and only if it contains a nonlinear worldline vertex*. From this perspective the above-mentioned issue with using dressed WL-NL vertices is all the better since there is no need for dressing—all diagrams with NL-WL vertices are factoriz-

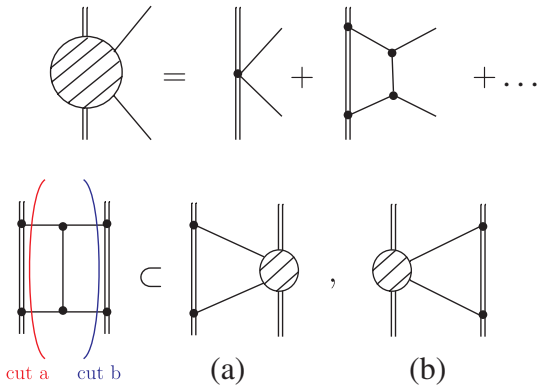

FIG. 14 (color online). The top line shows a possible definition for a 2-field dressed worldline vertex. The second line demonstrates the overcounting problem which occurs. The bare diagram on the left can be cut into subdiagrams in two different ways denoted (a) and (b).

[7]Except for the tree diagram limit of course.

[8]"From the point of view of making a practical calculation we have accomplished little; the unknown quantities ... have been expressed in terms of yet another unknown..." [36], "... the system involves an infinite hierarchy of equations ... their usefulness is limited" [37].

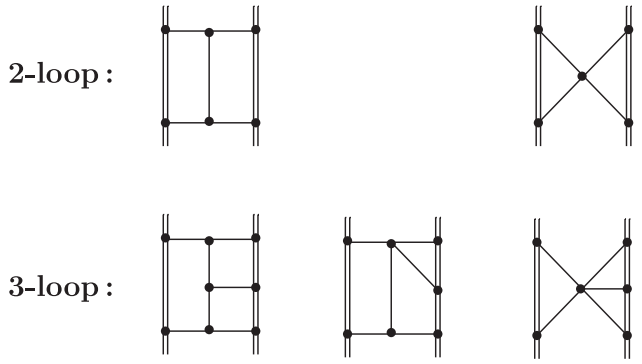

FIG. 15. Classification of topologies for irreducible diagrams of the 2-body effective action, both nonfactorizable and dressing-irreducible. The top line shows the possibilities at 2-loop, and the bottom line shows the possibilities at 3-loop.

able and hence reduce to computations of lower order and lower loop number.

It is interesting to *classify the possible irreducible diagrams in the 2-body effective action*—those which are both nonfactorizable and dressing-irreducible. The possible topologies are independent of the details of the specific field theory. At 1-loop there are no irreducible diagram topologies. At 2-loop (top line of Fig. 15) there is the "H" diagram on the left and its degeneration—the "X" diagram where the two cubic bulk vertices degenerate into a quartic vertex. At 3-loop (bottom line of Fig. 15) there is the topology shown on the left, together with its two possible degenerations. We did not list here the trivial 0-loop (tree-level) diagram shown in Fig. 1.

III. DRESSING THE 2-BODY POST-NEWTONIAN PROBLEM

In this section we apply the dressed perturbation theory to the post-Newtonian expansion, thereby demonstrating its utility. We start in Sec. III A by setting up the problem, establishing the conventions, and displaying the post-Newtonian effective action and the associated Feynman rules. In Sec. III B we explicitly compute the three PN charges both in k space and in position space up to the order required to reproduce the 2PN results, apart from the stress that is determined to one additional order. In Sec. III C we analyze qualitatively the diagrams relevant to the computation of the two-body effective action including a list of all the skeletons required for the computation of 3PN. In Sec. III D we compute certain novel 3PN and 4PN diagrams.

A. Effective action and Feynman rules

Consider a binary system composed of slowly moving massive objects. Replacing the vicinity of each of these objects by the relativistic point particle coupled to gravity and neglecting the effects of the higher-dimensional tidal terms, leads to the following effective action

$$S = S_{\rm EH} + S_{pp}. \tag{3.1}$$

In PN the gravitational metric field is naturally divided into three fields of nonrelativistic gravity (NRG fields): ϕ the Newtonian potential, A_i the gravitomagnetic vector potential and γ_{ij} a symmetric tensor (with spatial indices) [8]. The field redefinition $g_{\mu\nu} \to (\phi, A_i, \gamma_{ij})$ is defined by [7–9]

$$\begin{aligned} ds^2 &= g_{\mu\nu}dx^\mu dx^\nu \\ &= e^{2\phi}(dt - A_i dx^i)^2 - e^{-2\phi/(d-3)}\gamma_{ij}dx^i dx^j, \end{aligned} \tag{3.2}$$

where we take the space-time dimension d to be arbitrary and only at the end we shall specialize to 4D. The bulk action is the Einstein-Hilbert action expressed in terms of NRG fields

$$S_{\rm EH}[g] = \frac{1}{16\pi G}\int R[g] \to S_{\rm EH}[\gamma, A, \phi]. \tag{3.3}$$

The point-particle trajectory is denoted by $\vec{x} = \vec{x}(t)$ and we shall denote by $\vec{v} = \dot{\vec{x}}(t)$ and $\vec{a} = \ddot{\vec{x}}(t)$ its 3-velocity and 3-acceleration, respectively. The point-particle action is given by

$$\begin{aligned} S_{pp} &= -\sum_a m_a \int d\tau \\ &= -\sum_a m_a \int dt e^{\phi} \\ &\quad \times \sqrt{(1-\vec{A}\cdot\vec{v}_a)^2 - e^{-2(d-2)\phi/(d-3)}\gamma_{ij}v_a^i v_a^j} \\ &= -\sum_a m_a \int dt\sqrt{1-v_a^2} - \sum_a m_a \int dt\Big(\frac{(d-3)+v_a^2}{(d-3)\sqrt{1-v_a^2}} \\ &\quad \times \phi - \frac{\vec{A}\cdot\vec{v}_a}{\sqrt{1-v_a^2}} - \frac{\sigma_{ij}v_a^i v_a^j}{2\sqrt{1-v_a^2}} + \cdots\Big), \end{aligned} \tag{3.4}$$

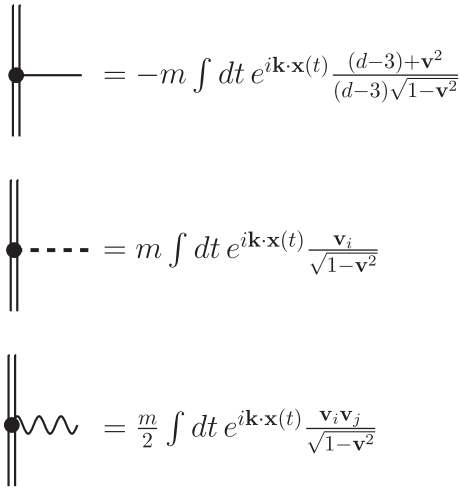

FIG. 16. Feynman rules obtained from the expansion of (3.4) up to linear order in ϕ, A_i and σ_{ij}. The undetermined wave numbers flow into the vertex.

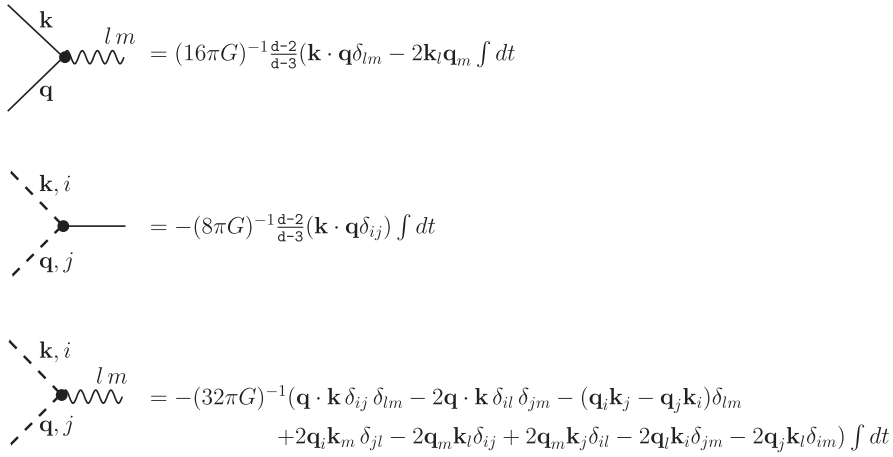

FIG. 17. Static bulk vertices obtained from the expansion of the Hilbert-Einstein action (3.3) and gauge fixing term (3.6) but restricting to time-independent terms. The undetermined wave numbers flow into the vertex.

where the dummy index a runs over all the masses involved in the binary evolution, in the second equality Eq. (3.2) was applied, the ellipsis denote terms nonlinear in the bulk fields (ϕ, A, γ) and we define

$$\sigma_{ij} := \gamma_{ij} - \delta_{ij}. \tag{3.5}$$

The Einstein-Hilbert action is invariant under reparametrizations and should be gauge fixed. Leaving aside the question which gauge would be optimal for this problem, we choose the harmonic gauge in order to facilitate comparison with the literature. Accordingly, we add the following gauge fixing term to the Einstein-Hilbert action

$$S_{\rm GF} = \frac{1}{32\pi G}\int d^dx\sqrt{g}\Gamma^\mu\Gamma^\nu g_{\mu\nu}, \tag{3.6}$$

where $\Gamma^\mu = \Gamma^\mu_{\alpha\beta}g^{\alpha\beta}$.

The Feynman rules for ϕ, A_i and σ_{ij} coupled to the worldline can be read from (3.4) and we list on Fig. 16 those couplings which are necessary to our discussion. Solid lines, dashed lines and wavy lines of the figure are associated with propagators of the instantaneous nonrelativistic modes ϕ, A_i and σ_{ij}, respectively. In momentum space these propagators are given by

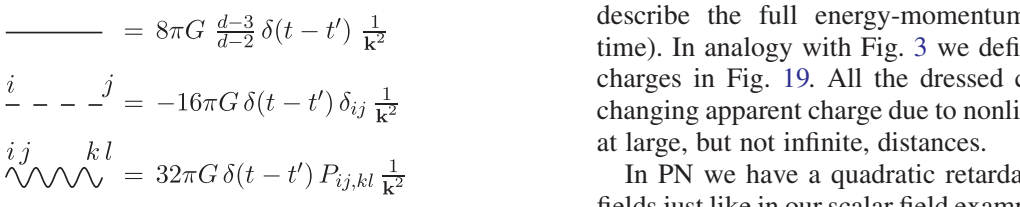

with $P_{ij,kl} = \frac{1}{2}[\delta_{ik}\delta_{jl} + \delta_{il}\delta_{jk} - \frac{2}{d-3}\delta_{ij}\delta_{kl}]$.

The Feynman rules for the bulk vertices are obtained from expansion of the Einstein-Hilbert action (3.3) and the gauge fixing term (3.6). The resulting set of vertices which contribute to the calculations below are presented in Figs. 17 and 18, where we separate vertices which involve time derivatives in Fig. 18, from the static ones in Fig. 17.

In addition, one has to impose wave number[9] conservation at each bulk vertex by assigning it a delta-function factor, $(2\pi)^{d-1}\delta(\sum_i \mathbf{k}_i)$, where $\sum_i \mathbf{k}_i$ is the total wave number flow into a given vertex, and one must integrate over each undermined wave number $\mathbf{k}$ of the diagram

$$\int_{\mathbf{k}} := \int\frac{d^{d-1}\mathbf{k}}{(2\pi)^{d-1}}. \tag{3.7}$$

Finally, one has to divide by the symmetry factor of the diagram.

B. Dressed charges

Given the general theory, it is natural to inquire about the form of the dressed quantities within PN. Accordingly we would like to compute the dressed charges (the dressed propagators are simple and are also discussed below).

Following our discussion at the end of Sec. II B on the generalization of the definitions for dressed subdiagrams to a multifield field theory we define three dressed charges for the interaction of gravity with a compact pointlike object. The ϕ charge is usually referred to as energy, the A charge is the energy current (or alternatively, momentum distribution) and the σ charge is the stress. Together they describe the full energy-momentum tensor (in spacetime). In analogy with Fig. 3 we define the 3 dressed PN charges in Fig. 19. All the dressed charges describe the changing apparent charge due to nonlinear bulk interaction at large, but not infinite, distances.

In PN we have a quadratic retardation vertex for all 3 fields just like in our scalar field example. Since the 3 fields have different tensor characters they cannot mix, and we have exactly 3 dressed propagators each one defined as in Fig. 7 (bottom). Physically they all correspond to full

[9]Quantum mechanically the wave number k is equivalent to momentum, and this is how k is usually referred to, but in classical field theory it is not a momentum.

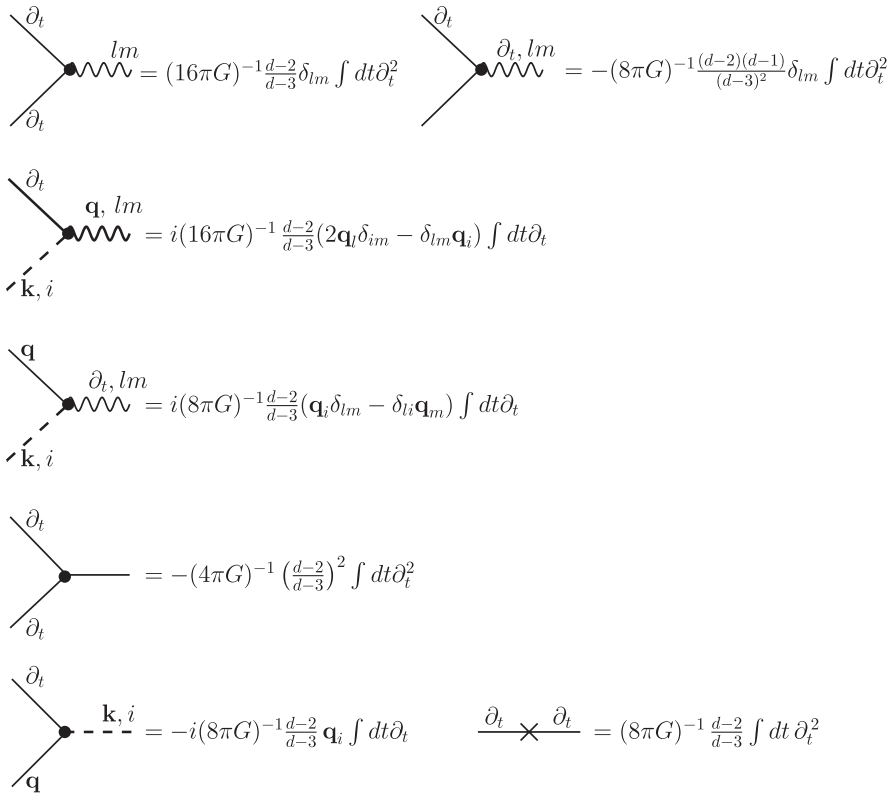

FIG. 18. Time-dependent bulk vertices obtained from the expansion of the Hilbert-Einstein action (3.3) and gauge fixing term (3.6). Time derivative above the propagator indicates the direction on which it acts. The undetermined wave numbers flow into the vertex.

relativistic propagators, even though A and σ are spatial rather than space-time tensors.

The Feynman diagrams required for the computation of the dressed energy distribution, ρ,[10] and the stress, s^{ij}, up to 2PN as well as the dressed momentum distribution, j^i, up to 1.5PN are shown in Figs. 20–22.[11] The PN order was chosen as the one required for the 2PN effective action, except for the case of the stress where we chose to compute an additional PN order. All the results below apart from the last term of the dressed stress 2PN were tested and confirmed against the known expression for 2PN effective action. In addition we shall show in the next subsections how to use the dressed charges to calculate diagrams beyond 2PN.

Given the Feynman rules of the previous subsection, one can write down the expressions for the Feynman integrals. The integrals which are essential for the evaluation of the loop integrals and the Fourier transforms are listed in the appendix. Note also that since we compute the dressed sources up to a definite order in the PN expansion there is no need to keep the vertices of Fig. 16 as they are. Instead, one has to expand each such vertex keeping only those powers of "v" which contribute to the PN order under consideration.

We proceed to present the results of all the diagrams. We start from the dressed energy distribution. Let us denote

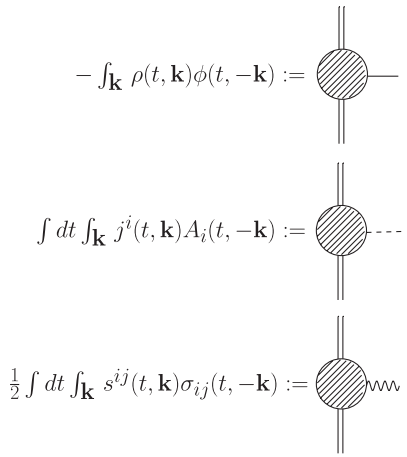

FIG. 19. The diagrammatic definition of the dressed charge distributions in PN ρ, j^i and s^{ij} as the one point function for ϕ, A_i and σ_{ij} respectively in the presence of a single source. Retardation vertices are forbidden from the external leg.

[10] In this section we shall shorten the notation and write ρ rather than ρ_{dr}.

[11] Alternatively, one may count PN orders relative to the leading order. With this convention the dressed energy is computed to order +2PN relative to leading, while the dressed momentum and stress are computing to +1PN beyond leading.

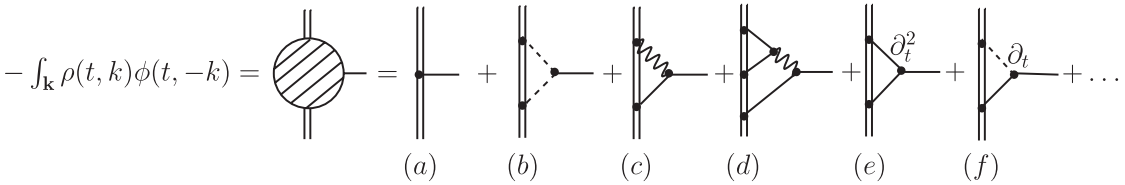

FIG. 20. Feynman diagrams which contribute to the dressed energy distribution up to 2PN. Diagram (a) is leading (order 0PN) while the rest are 2PN.

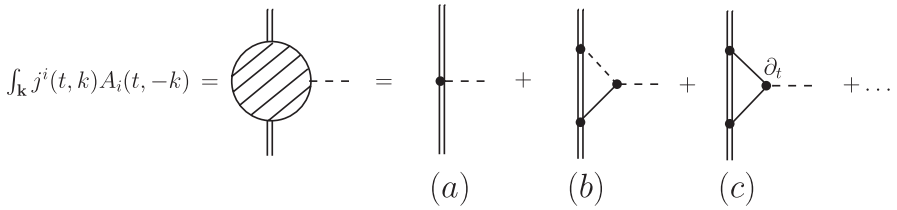

FIG. 21. Feynman diagrams which contribute to the dressed momentum distribution up to 1.5PN. Diagram (a) is leading (order 0.5PN) while the rest are +1PN (1.5PN).

$$\lambda := Gm^2 \frac{\Gamma((3-d)/2)\Gamma((d-1)/2)}{(16\pi)^{(d-4)/2}\Gamma(d/2)}, \tag{3.8}$$

then

$$\text{Fig. } 20(\text{a}) = -m\int dt \frac{(d-3)+v^2}{(d-3)\sqrt{1-v^2}}\phi(t,\vec{x}(t))$$
$$\Rightarrow \delta\rho(t,\vec{x}) = m\left(1+\frac{d-1}{2(d-3)}v^2+\frac{3d-5}{8(d-3)}v^4\right)\delta(\vec{x}-\vec{x}(t)),$$
$$\delta\rho(t,\vec{k}) = m\left(1+\frac{d-1}{2(d-3)}v^2+\frac{3d-5}{8(d-3)}v^4\right) \times \exp(-i\vec{k}\cdot\vec{x}(t)), \tag{3.9}$$

$$\text{Fig. } 20(\text{b}) = \lambda\frac{(d-2)^2}{2(d-3)}\int dt\vec{v}^2 \times \int_{\mathbf{k}} e^{-i\vec{k}\cdot\vec{x}(t)}|\vec{k}|^{d-3}\phi(t,-\vec{k}) \tag{3.10}$$

$$\text{Fig. } 20(\text{c}) = \lambda\frac{d-2}{2}\int dt \times \int_{\mathbf{k}} e^{-i\vec{k}\cdot\vec{x}(t)}|\vec{k}|^{d-5}(\vec{k}\cdot\vec{v})^2\phi(t,-\vec{k}) \tag{3.11}$$

$$\text{Fig. } 20(\text{d}) = \frac{(16\pi G)^2m^3}{24}\frac{(d-3)^2}{(d-2)(d-5)} \times \int dt\int_{\mathbf{k}} e^{-i\vec{k}\cdot\vec{x}(t)}\vec{k}^2 I(|\vec{k}|)\phi(t,-\vec{k})$$
$$\Rightarrow \delta\rho(t,\vec{k}) = -\frac{(16\pi G)^2m^3}{24} \times \frac{(d-3)^2}{(d-2)(d-5)}e^{-i\vec{k}\cdot\vec{x}(t)}\vec{k}^2 I(|\vec{k}|), \tag{3.12}$$

with

$$I(|\vec{k}|) = \sqrt{\pi}\frac{\Gamma(4-d)}{(4\pi)^{d-1}}\frac{\Gamma(d/2-3/2)^2\Gamma(d-3)}{\Gamma(d/2-1)\Gamma(3d/2-9/2)} \times \left(\frac{\vec{k}^2}{2}\right)^{d-4}. \tag{3.13}$$

Apparently, the above expression possesses a pole when $d=4$, and thus one needs to introduce a counterterm which inevitably leads to a logarithmic behavior of the dressed energy distribution with scale. Yet this pole is unphysical. Indeed, applying a Fourier transform to Eq. (3.12) yields

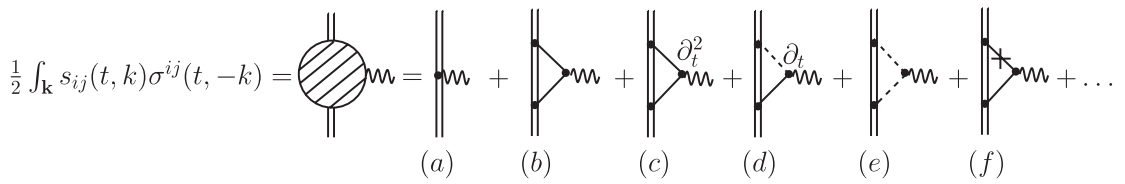

FIG. 22. Feynman diagrams which contribute to the dressed stress tensor distribution up to 2PN. Diagrams (a),(b) are leading (order 1PN) while the rest are +1PN (2PN).

$$\delta\rho(t,\vec{r}) = (8\pi G)^2\left(\frac{m}{\Omega_{d-2}}\right)^3 \frac{(d-3)}{(d-2)(d-5)}|\vec{r}|^{7-3d}, \tag{3.14}$$

where

$$\Omega_{d-2} = \frac{2\pi^{(d-1)/2}}{\Gamma((d-1)/2)}, \qquad \vec{r} = \vec{x} - \vec{x}(t), \tag{3.15}$$

and this expression is regular for $d = 4$.

Alternatively, one could stay within the wave number space (k space) by introducing the following counterterm

$$\begin{aligned} \text{ct} &= -\frac{G^2m^3}{6(d-4)}\int dt \int_{\mathbf{k}} e^{-i\vec{k}\cdot\vec{x}(t)}\vec{k}^2\phi(t,-\vec{k}) \\ &= \frac{G^2m^3}{6(d-4)}\int dt \Box\phi(t,\vec{x}(t)). \end{aligned} \tag{3.16}$$

However, as explained in [5] such a term can be removed from the Lagrangian by an appropriate field redefinition as it is proportional to the leading order equation of motion for the NRG field ϕ and hence it is a redundant term.[12]

The contribution to the energy distribution of the diagrams which contain time derivatives is given by

$$\begin{aligned} \text{Fig. 20(e)} &= -\frac{\lambda}{8}\int dt \int_{\mathbf{k}} e^{-i\vec{k}\cdot\vec{x}(t)}|\vec{k}|^{d-5}[\vec{k}^2\vec{v}^2 - (3d-5) \\ &\quad \times (\vec{k}.\vec{v})^2 - 4(d-2)(i\vec{k}\cdot\vec{a})]\phi(t,-\vec{k}) \\ \text{Fig. 20(f)} &= -\frac{d-2}{2}\lambda\int dt \int_{\mathbf{k}} e^{-i\vec{k}\cdot\vec{x}(t)}|\vec{k}|^{d-5} \\ &\quad \times [i\vec{k}\cdot\vec{a} + 2(\vec{k}\cdot\vec{v})^2]\phi(t,-\vec{k}) \end{aligned} \tag{3.17}$$

Combining altogether we get up to 2PN

$$\begin{aligned} \rho(t,\vec{k})e^{i\vec{k}\cdot\vec{x}(t)} &= m\left(1 + \frac{d-1}{2(d-3)}v^2 + \frac{3d-5}{8(d-3)}v^4\right) \\ &\quad - \frac{(16\pi G)^2m^3}{24}\frac{(d-3)^2}{(d-2)(d-5)}\vec{k}^2 I(|\vec{k}|) \\ &\quad - \frac{4d^2-17d+19}{8(d-3)}\lambda|\vec{k}|^{d-3}v^2 \\ &\quad + \frac{d-3}{8}\lambda|\vec{k}|^{d-5}(\vec{k}\cdot\vec{v})^2, \end{aligned} \tag{3.18}$$

where the exponential on the left-hand side really belongs on the right-hand side and was moved from there to achieve a "cleaner" form. Transforming back to coordinate space yields

$$\begin{aligned} \rho(t,\vec{r}) &= m\left(1 + \frac{d-1}{2(d-3)}v^2 + \frac{3d-5}{8(d-3)}v^4\right)\delta(\vec{r}) \\ &\quad + 8\pi G\left(\frac{m}{\Omega_{d-2}}\right)^2\left[(\vec{v}\cdot\hat{r})^2 - 2\frac{d-2}{d-3}v^2\right]|\vec{r}|^{4-2d} \\ &\quad + (8\pi G)^2\left(\frac{m}{\Omega_{d-2}}\right)^3\frac{(d-3)}{(d-2)(d-5)}|\vec{r}|^{7-3d}. \end{aligned} \tag{3.19}$$

The results for the dressed momentum distribution up to 1.5PN are

$$\begin{aligned} \text{Fig. 21(a)} &= \int dt \frac{mv^i}{\sqrt{1-v^2}}A_i(t,\vec{x}(t)) \\ \Rightarrow dj^i(t,\vec{x}) &= mv^i\left(1 + \frac{1}{2}v^2\right)\delta(\vec{x} - \vec{x}(t)), \\ \delta j^i(t,\vec{k}) &= mv^i\left(1 + \frac{1}{2}v^2\right)\exp(-i\vec{k}\cdot\vec{x}(t)), \\ \text{Fig. 21(b)} &= -\lambda\frac{d-2}{2}\int dt \int_{\mathbf{k}} e^{-i\vec{k}\cdot\vec{x}(t)}|\vec{k}|^{d-3}\vec{v}\cdot\vec{A}(t,-\vec{k}) \\ \text{Fig. 21(c)} &= -\lambda\frac{d-3}{8(d-2)}\int dt \int_{\mathbf{k}} e^{-i\vec{k}\cdot\vec{x}(t)}|\vec{k}|^{d-5}(\vec{k}^2v_i \\ &\quad + (d-3)(\vec{k}\cdot\vec{v})k_i)A^i(t,-\vec{k}). \end{aligned} \tag{3.20}$$

Altogether we obtain up to 1.5PN

$$\begin{aligned} j^i(t,\vec{k})e^{i\vec{k}\cdot\vec{x}(t)} &= mv^i\left(1 + \frac{1}{2}v^2\right) \\ &\quad - \frac{4d^2-17d+19}{8(d-2)}\lambda|\vec{k}|^{d-3}v^i \\ &\quad + \frac{(d-3)^2}{8(d-2)}\lambda|\vec{k}|^{d-5}(\vec{k}\cdot\vec{v})k^i. \end{aligned} \tag{3.21}$$

In coordinate space the dressed momentum distribution is

$$\begin{aligned} j^i(t,\vec{r}) &= mv^i\left(1 + \frac{1}{2}v^2\right)\delta(\vec{r}) + 8\pi G\left(\frac{m}{\Omega_{d-2}}\right)^2 \\ &\quad \times\left[\frac{d-3}{d-2}(\vec{v}\cdot\hat{r})\hat{r}^i - 2v^i\right]|\vec{r}|^{4-2d}. \end{aligned} \tag{3.22}$$

Finally, the results for the dressed stress charge up to 2PN are given by

$$\begin{aligned} \text{Fig. 22(a)} &= \frac{m}{2}\int dt \frac{v^iv^j}{\sqrt{1-v^2}}\sigma_{ij}(t,\vec{x}) \\ \Rightarrow \delta s^{ij}(t,\vec{x}) &= mv^iv^j\left(1 + \frac{1}{2}v^2\right)\delta(\vec{x} - \vec{x}(t)), \\ \delta s^{ij}(t,\vec{k}) &= mv^iv^j\left(1 + \frac{1}{2}v^2\right)\exp(-i\vec{k}\cdot\vec{x}(t)), \end{aligned} \tag{3.23}$$

[12] In quantum field theory such an object is called a redundant *operator* referring to its action on the Hilbert space of states. In the classical theory it is not an operator and calling it a *term* is more appropriate.

$$\text{Fig. 22(b)} = -\lambda\frac{(d-3)^2}{16(d-2)}\int dt\left(1+\frac{d-1}{d-3}v^2\right)\times\int_{\mathbf{k}} e^{-i\vec{k}\cdot\vec{x}(t)}|\vec{k}|^{d-5}[k_ik_j-\vec{k}^2\delta_{ij}]\sigma^{ij}(t,-\vec{k}) \tag{3.24}$$

$$\text{Fig. 22(c)} = \lambda\frac{d-3}{32(d-2)}\int dt\int_{\mathbf{k}} e^{-i\vec{k}\cdot\vec{x}(t)}|\vec{k}|^{d-5}\left[\frac{(3d-5)^2}{d-3}\times(\vec{k}\cdot\vec{v})^2+\vec{k}^2\vec{v}^2+\frac{8(d-1)(d-2)}{d-3}i\vec{k}\cdot\vec{a}\right]\times\delta_{ij}\sigma^{ij}(t,-\vec{k}) \tag{3.25}$$

$$\text{Fig. 22(d)} = \lambda\frac{d-2}{2}\int dt\int_{\mathbf{k}} e^{-i\vec{k}\cdot\vec{x}(t)}|\vec{k}|^{d-5}\left[\frac{1}{2}(\vec{k}\cdot\vec{v})^2\delta_{ij}+(i\vec{k}\cdot\vec{a})\delta_{ij}-ik_ia_j\right]\sigma^{ij}(t,-\vec{k}) \tag{3.26}$$

$$\text{Fig. 22(e)} = \frac{\lambda}{8}\int dt\int_{\mathbf{k}} e^{-i\vec{k}\cdot\vec{x}(t)}|\vec{k}|^{d-5}\left[(d-3)(\vec{k}^2\vec{v}^2\delta_{ij}-\vec{v}^2k_ik_j)-2(d-2)\vec{k}^2v_iv_j\right]\sigma^{ij}(t,-\vec{k}) \tag{3.27}$$

$$\begin{aligned}\text{Fig. 22(f)} = &-\frac{\lambda}{4}\frac{d-3}{d-2}\int dt\int_{\mathbf{k}} e^{-i\vec{k}\cdot\vec{x}(t)}|\vec{k}|^{d-5}\left[\frac{d-2}{8}\vec{k}^2\vec{v}^2-\frac{(d-3)(d-4)}{8}(\vec{k}\cdot\vec{v})^2-\frac{d^2-7d+11}{4}(i\vec{k}\cdot\vec{a})\right]\delta_{ij}\sigma^{ij}(t,-\vec{k})\\ &-\frac{\lambda}{4}\frac{d-3}{d-2}\int dt\int_{\mathbf{k}} e^{-i\vec{k}\cdot\vec{x}(t)}|\vec{k}|^{d-5}\left[-\frac{d-3}{8}\vec{v}^2k_ik_j+\frac{(d-3)(d-5)}{8}(\hat{k}\cdot\vec{v})^2k_ik_j-\frac{1}{4}\vec{k}^2v_iv_j\right]\sigma^{ij}\\ &-\frac{\lambda}{4}\frac{d-3}{d-2}\int dt\int_{\mathbf{k}} e^{-i\vec{k}\cdot\vec{x}(t)}|\vec{k}|^{d-5}\left[-\frac{ik_ia_j}{2}+\frac{(d-3)(d-5)}{4}(\vec{k}\cdot\vec{a})i\hat{k}_i\hat{k}_j\right]\sigma^{ij}\end{aligned} \tag{3.28}$$

As a result, the dressed stress charge up to 2PN is given by

$$\begin{aligned}s^{ij}(t,\vec{k})e^{i\vec{k}\cdot\vec{x}(t)} = &\,mv^iv^j\left(1+\frac{1}{2}v^2\right)-\frac{4d^2-17d+19}{4(d-2)}\left(ik^{(i}a^{j)}+\frac{\vec{k}^2}{2}v^iv^j\right)|\vec{k}|^{d-5}\lambda+\frac{(d-3)^2}{8(d-2)}\left(1-\frac{v^2}{2}-\frac{d-5}{2}(\vec{v}\cdot\hat{k})^2\right.\\ &\left.-(d-5)\frac{i\vec{a}\cdot\vec{k}}{\vec{k}^2}\right)k^ik^j|\vec{k}|^{d-5}\lambda+\left[\frac{(d-1)(d^2+8d-21)}{16(d-2)}(\vec{k}\cdot\vec{v})^2+\frac{d^3+2d^2-12d+7}{8(d-2)}i\vec{a}\cdot\vec{k}\right]|\vec{k}|^{d-5}\lambda\delta^{ij}\\ &-\frac{(d-3)^2}{8(d-2)}\left(1-\frac{v^2}{2}\right)|\vec{k}|^{d-3}\lambda\delta^{ij},\end{aligned} \tag{3.29}$$

where (ij) denotes symmetrization with respect to indices i and j with factor $1/2$ included. In the coordinate space we obtain

$$\begin{aligned}s^{ij}(t,\vec{r}) = &\,mv^iv^j\left(1+\frac{1}{2}v^2\right)\delta(\vec{r})-\frac{(3d-5)}{(d-2)(d-3)}f(r)\vec{r}^{(i}a^{j)}-2f(r)v^iv^j-\frac{d^2+10d-15}{4(d-2)(d-3)}f(r)(v^2-2(d-2)(\vec{v}\cdot\hat{r})^2)\delta^{ij}\\ &-\frac{d-3}{d-2}f(r)\left((d-1)(\vec{v}\cdot\hat{r})^2\hat{r}^i\hat{r}^j-2(\vec{v}\cdot\hat{r})v^i\hat{r}^j+\frac{1}{2}\left(1-\frac{v^2}{2}\right)\delta^{ij}-\hat{r}^i\hat{r}^j+(\vec{a}\cdot\vec{r})\hat{r}^i\hat{r}^j\right)\\ &+\frac{d^2+5d-8}{2(d-2)(d-3)}f(r)(\vec{a}\cdot\vec{r})\delta^{ij},\end{aligned} \tag{3.30}$$

with

$$f(r)=\frac{8\pi G}{|\vec{r}|^{2d-4}}\left(\frac{m}{\Omega_{d-2}}\right)^2. \tag{3.31}$$

C. Skeletons for 2PN and 3PN

We shall now demonstrate how all the bare diagrams of the two-body effective action up to 2PN, order by order transform into their dressed form, including their corresponding skeletons.

At 0PN (Newtonian order) a single diagram (Fig. 1) contributes representing the interaction of two tree-level masses.

At 1PN (Einstein-Infeld-Hoffmann Lagrangian) the four diagrams shown in Fig. 23 contribute. The first is a v^2 component of the mass vertex and can be considered to be a trivial dressing of the energy. The second is the tree-level interaction of two currents. The third represents a propagator dressing (retardation) of the Newtonian potential. Finally the fourth is due to a nonlinear worldline vertex which accounts for the gravitating nature of potential energy. Altogether none is irreducible with a topology other than Newtonian. We note that the last diagram is of order $\mathcal{O}(G^2m^3v^0)$ where m represents a typical mass and v a typical velocity while all the previous diagrams are of order $\mathcal{O}(Gm^2v^2)$.

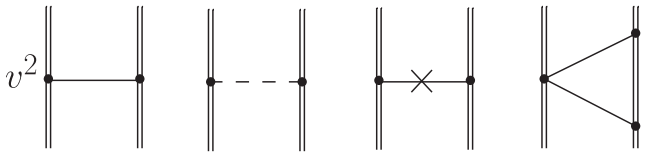

FIG. 23. The four diagrams which contribute to the two-body effective action at 1PN—the Einstein-Infeld-Hoffmann Lagrangian.

At 2PN Gilmore and Ross [9] found 21 diagrams. We shall see that many can be interpreted to represent dressing effects while only one is both nonfactorizable and dressing-irreducible. Indeed [9] find its computation to be the core or essential computation at this order.

The six diagrams shown in Figs. 24(a)–24(f) contribute at order $\mathcal{O}(Gm^2v^4)$. Figures 24(b), 24(c), and 24(e) represent propagator dressing to diagrams from lower orders, while the rest involve only tree-level v-dependent vertices.

At order $\mathcal{O}(G^2m^3v^2)$ there are 10 diagrams shown in Fig. 25. Figures 25(a)–25(c) are V-shaped and as such factorizable and at least one factor is the Newtonian potential. Figures 25(d)–25(j) are Y-shaped and as such are dressing-reducible. Four diagrams [25(d), 25(f), 25(g), and 25(i)]) represent mass dressing, the two [25(e) and 25(h)] represent current dressing, while finally [25(j)] can be thought to represent stress dressing.

At order $\mathcal{O}(G^3m^4v^0)$ there are 5 diagrams. Both [26(a) and 26(c)] factorize into 3 Newtonian-potential factors. Figure 26(b) represents a mass dressing (the circled piece) while 26(e) includes two σ dressing subdiagrams. Finally diagram 26(d) is the one and only truly irreducible diagram at 2PN. Actually for some yet-unexplained reason the computation reduces after several steps to a square of the master one-loop integral. We speculate that this is special to the GR action (and is not generic to classical field theories) and in particular to the gauge symmetry which may relate this diagram to other diagrams at 2PN.

As a result of this analysis we can extract all the nonfactorizable skeletons up to 2PN. These are listed in Fig. 27, where the skeletons are labeled according to the PN order in which they first appear. By evaluating the dressed diagrams we successfully tested our expressions for the dressed charges from the previous subsection against the known expressions for the effective action.

3PN. As a step towards the determination of 3PN we extend the list of skeletons up to that order using the classification of possible topologies in Fig. 15 and some knowledge on the Feynman rules of PN. Taken together with the evaluation of the dressed vertices (partially obtained in the last subsection) this list of skeletons leads the way to a determination of the 3PN part of the 2-body effective action. We note that the 3-loop topologies of Fig. 15 are *not* realized at 3PN. The reason is the absence in PN of certain bulk vertices such as ϕ^3.

D. Computing beyond 2PN

In this subsection we explicitly demonstrate the economizing ability of the proposed approach in several cases

(i) A certain economization during 2PN calculation.
(ii) Using the dressed energy distribution computed above in Sec. III B to calculate terms of the Newtonian interaction type of order 3PN and 4PN.
(iii) Similarly, using the computed dressed momentum distributions we calculate a current-current interaction term of order 3PN.
(iv) Finally, we use our highest order results for the dressed stress in order to compute 3PN terms by attaching the external σ leg to the second compact object.

An application at 2PN. The first nontrivial example appears during the computation of the 2-body effective Lagrangian at order 2PN. Indeed the dressed stress subdiagram in Fig. 22(b) appears twice at 2PN—both at Fig. 25(j) and at Fig. 26(b), and of course it is enough to evaluate it once. Another point of view is to obtain both dressed energies corresponding to Figs. 20(c) and 20(d) from the recursive relation shown in Fig. 28 after substituting in the leading contribution to the dressed stress from Figs. 22(a) and 22(b).

Proceeding *beyond 2PN* we shall now compute certain 3PN and 4PN terms in the 2-body effective action building on the results of the previous section. Pictorially these terms are shown on Fig. 29, where the bubbles represent the dressed charges, and we explicitly indicate on each bubble which piece of the dressed charge is essential to the computation.

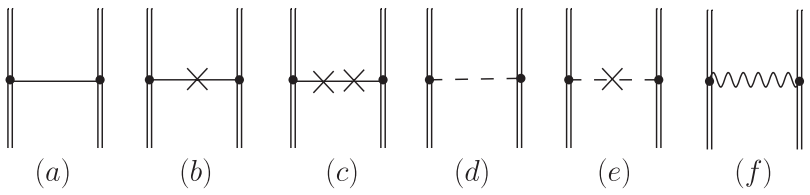

FIG. 24. 2PN Diagrams contributing at order $\mathcal{O}(Gm^2v^4)$ (following [9]).

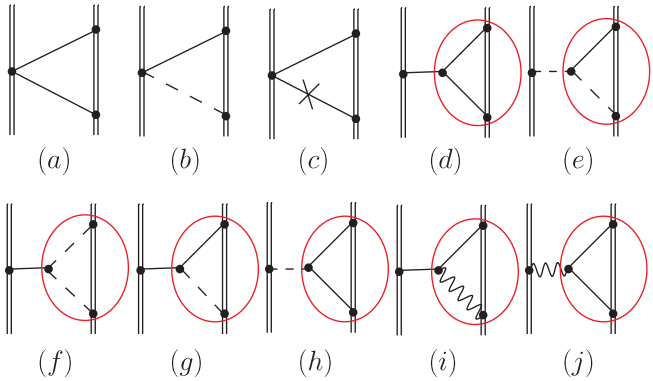

FIG. 25 (color online). 2PN Diagrams contributing at order $\mathcal{O}(G^2m^3v^2)$ (following [9]).

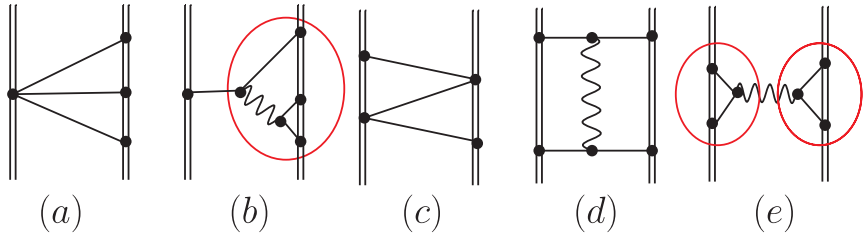

FIG. 26 (color online). 2PN Diagrams contributing at order $\mathcal{O}(G^3m^4v^0)$ (following [9]).

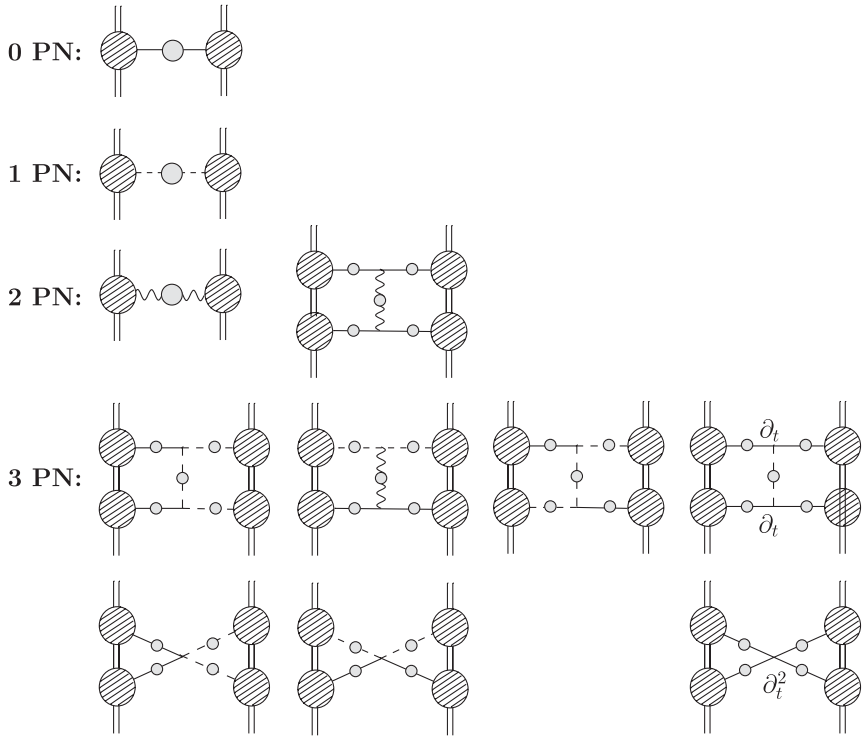

FIG. 27. A listing of all nonfactorizable skeletons appearing in the dressed post-Newtonian perturbation theory up to 3PN, listed by the PN order at which they first appear.

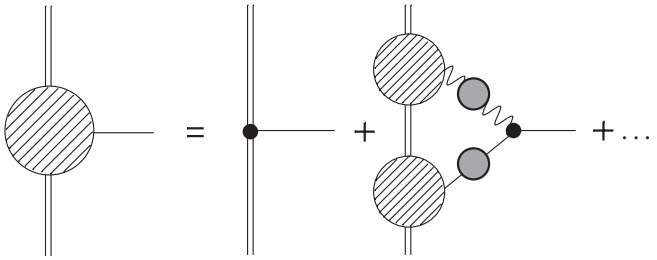

FIG. 28. The diagrammatic representation of the recursive integral equation satisfied by the dressed energy.

Building on the Feynman rules of the previous section, we obtain

$$\text{Figs. 29(a), (29d)} = 8\pi G\frac{d-3}{d-2} \times \int dt \int_{\mathbf{k}} \frac{\rho_2(t,-\vec{k})\rho_1(t,\vec{k})}{\vec{k}^2}, \tag{3.32}$$

$$\text{Fig. 29(b)} = -16\pi G \int dt \int_{\mathbf{k}} \frac{\vec{j}_2(t,-\vec{k}).\vec{j}_1(t,\vec{k})}{\vec{k}^2}, \tag{3.33}$$

$$\text{Fig. 29(c)} = 8\pi G \int dt \int_{\mathbf{k}} \frac{s_2^{ij}(t,-\vec{k})P_{ij,kl}s_1^{kl}(t,\vec{k})}{\vec{k}^2}. \tag{3.34}$$

The 3PN j-j and s-s terms. Substituting (3.21) and (3.29) and $d = 4$ into (3.33) and (3.34) yields

$$\begin{aligned}\text{Fig. 29(b)} = &-\int dt \frac{Gm_1m_2}{r}(\vec{v}_1\cdot\vec{v}_2)v_1^2v_2^2 - \int dt \frac{Gm_1m_2}{2r} \\ &\times\left(\frac{Gm_2}{r}v_1^2 + \frac{Gm_1}{r}v_2^2\right)[7(\vec{v}_1\cdot\vec{v}_2) + (\vec{v}_1\cdot\hat{r}) \\ &\times(\vec{v}_2\cdot\hat{r})] + \frac{7\pi^2}{32}\int dt \frac{G^3m_1^2m_2^2}{r^3}(\vec{v}_1\cdot\vec{v}_2 \\ &- 3(\vec{v}_1\cdot\hat{r})(\vec{v}_2\cdot\hat{r})),\end{aligned} \tag{3.35}$$

$$\begin{aligned}\text{Fig. 29(c)} = &\int dt \frac{Gm_1m_2}{r}[(\vec{v}_1\cdot\vec{v}_2)^2 - v_1^2v_2^2]v_1^2 + \int dt \frac{G^2m_1^2m_2}{r^2}\left[\frac{1}{2}(\vec{v}_1\cdot\vec{v}_2)^2 + \frac{203}{12}v_2^2v_1^2\right] \\ &+ \int dt \frac{G^2m_1^2m_2}{r^2}\left[-\frac{22}{3}(\vec{v}_2\cdot\vec{r})(\vec{a}_1\cdot\vec{v}_2) - \frac{121}{4}v_2^2(\vec{a}_1\cdot\vec{r}) - \frac{1}{6}(\vec{a}_1\cdot\vec{r})(\vec{v}_2\cdot\hat{r})^2\right] - \int dt \frac{G^2m_1^2m_2}{r^2}\left[\frac{245}{6}v_2^2(\vec{v}_1\cdot\hat{r})^2\right. \\ &\left.+ \frac{1}{4}v_1^2(\vec{v}_2\cdot\hat{r})^2 + \frac{1}{3}(\vec{v}_1\cdot\hat{r})^2(\vec{v}_2\cdot\hat{r})^2 + \frac{1}{12}(\vec{v}_1\cdot\vec{v}_2)^2\right] + \frac{1}{3}\int dt \frac{G^2m_1^2m_2}{r^2}[(\vec{v}_1\cdot\vec{v}_2)(\vec{v}_1\cdot\hat{r})(\vec{v}_2\cdot\hat{r})] + (1\leftrightarrow 2),\end{aligned} \tag{3.36}$$

where $\vec{r}(t) = \vec{x}_2(t) - \vec{x}_1(t)$ denotes the radius vector between the particles, and we have neglected the contact term proportional to $\delta(\vec{r})$ since in CLEFT particles are widely separated from each other.

The ρ-ρ terms. Let us now evaluate Fig. 29(b). First note that since Eq. (3.12) contains a simple pole in $d = 4$ one concludes that the integrand of (3.32) possesses a double pole, and thus in contrast to the previous case (3.14) a Fourier transform will not lead to a regular expression.

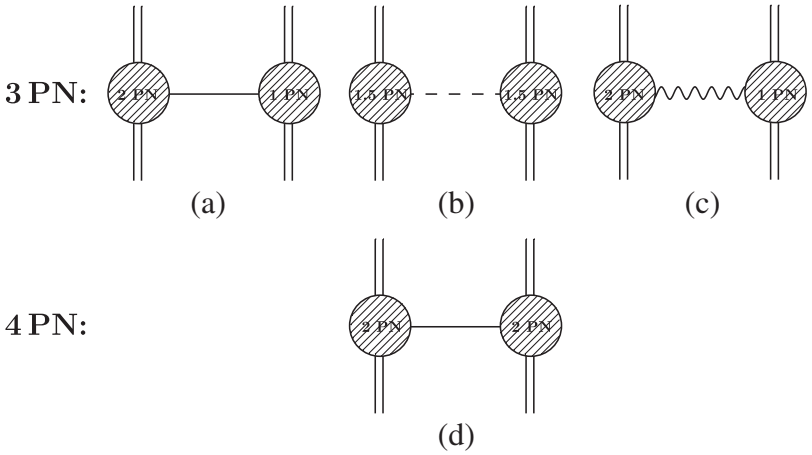

FIG. 29. The diagrammatic representation of terms beyond 2PN in the 2-body effective action: (a) a 3PN ρ-ρ term, (b) a 3PN j-j term, (c) a 3PN s-s term and finally (d) a 4PN ρ-ρ term.

Therefore, we expand Eq. (3.12) around $d = 4$

$$\text{Fig. 20(d)} = G^2 m_r^3 L^{-\epsilon} \int dt \int_{\mathbf{k}} e^{-i\vec{k}\cdot\vec{x}(t)} \vec{k}^2 \phi(t, -\vec{k}) \times \left[-\frac{1}{6\epsilon} + \frac{1}{12}(-1 + 2\gamma - 2\ln(8\pi^2) + 2\ln(\vec{k}^2 L^2)) + O(\epsilon) \right], \tag{3.37}$$

where γ is Euler's constant and motivated by the QFT renormalization approach we introduced an arbitrary length scale L and the following definitions[13]

$$\epsilon = 4 - d, \qquad Gm = G m_r L^{-\epsilon}. \tag{3.38}$$

In order to eliminate the divergence as $\epsilon \to 0$, we add the following counterterm to the effective action

$$\text{ct} = c \int dt \Delta\phi(t, \vec{x}(t)) = -c \int dt \int_{\mathbf{k}} e^{-i\vec{k}\cdot\vec{x}(t)} \vec{k}^2 \phi(t, -\vec{k}), \tag{3.39}$$

where

$$c = L^{-\epsilon}\left(c_r - \frac{G^2 m_r^3}{6\epsilon}\right). \tag{3.40}$$

Since the renormalization scale L introduced above is arbitrary, we must have

$$\begin{aligned} 0 = L\frac{dm}{dL} &= L^{-\epsilon}\left(-\epsilon m_r + L\frac{dm_r}{dL}\right) \\ \Rightarrow L\frac{dm_r}{dL} &= \epsilon m_r, \\ 0 = L\frac{dc}{dL} &= -\epsilon L^{-\epsilon}\left(c_r - \frac{G^2 m_r^3}{6\epsilon}\right) \\ &\quad + L^{-\epsilon}\left(L\frac{dc_r}{dL} - \frac{G^2 m_r^2}{2\epsilon} L\frac{dm_r}{dL}\right) \\ \Rightarrow L\frac{dc_r}{dL} &= \epsilon c_r + \frac{G^2 m_r^3}{3}. \end{aligned} \tag{3.41}$$

Apparently, the theory exhibits a nontrivial RG flow. But as argued in [5] this scaling is not physical in nature and can be removed by a suitable field redefinition which is tantamount to a coordinate transformation. Indeed, combining (3.37) with (3.39) yields

$$\delta\rho(t, \vec{k}) = \left[c_r - \frac{G^2 m_r^3}{12}(-1 + 2\gamma - 2\ln(8\pi^2) + 2\ln(\vec{k}^2 L^2)) \right] e^{-i\vec{k}\cdot\vec{x}(t)} \vec{k}^2. \tag{3.42}$$

In coordinate space this expression is given by

$$\delta\rho(t, \vec{r}) = \left[c_r - \frac{G^2 m_r^3}{12}(-1 + 2\gamma - 2\ln(8\pi^2)) \right] \delta(\vec{r}) - \frac{1}{2\pi}\frac{G^2 m_r^3}{r^5}, \tag{3.43}$$

where $\vec{r} = \vec{x} - \vec{x}(t)$ and the relation

$$\ln \vec{k}^2 = \lim_{\alpha \to 0} \frac{d}{d\alpha}(k^2)^\alpha \tag{3.44}$$

was used in order to apply the Fourier transform formulas of the appendix.

However, the contact term in the above expression for $\delta\rho$ can be eliminated by the following field redefinition

$$\phi \to \phi + 4\pi G\left[c_r - \frac{G^2 m_r^3}{12}(-1 + 2\gamma - 2\ln(8\pi^2)) \right] \delta(\vec{r}). \tag{3.45}$$

As a result, we reproduced Eq. (3.14) for $d = 4$ and also obtained the regularized expression for $\rho(t, \vec{k})$ in four dimensions[14]

$$\rho(t, \vec{k}) e^{i\vec{k}\cdot\vec{x}(t)} = m\left(1 + \frac{3}{2}v^2 + \frac{7}{8}v^4\right) + \frac{\pi}{8} G m^2 |\vec{k}| (15v^2 - (\hat{k}\cdot\vec{v})^2) - \frac{G^2 m^3}{6}\vec{k}^2 \ln(\vec{k}^2 L^2). \tag{3.46}$$

A comment should be made regarding the field redefinition (3.45). Obviously, such a shift introduces an extra term to the worldline action as a side effect. This term is proportional to the second derivative of the NRG field ϕ with respect to time. However, it can be removed by including additional counterterm given by

$$\text{ct} = \tilde{c} \int dt \frac{\partial^2 \phi}{\partial t^2}(t, \vec{x}(t)). \tag{3.47}$$

We will not elaborate the details of this elimination as they are irrelevant to the computation of the 4PN term.

Substituting (3.46) into (3.32) leads to

$$\text{Fig. 29(a)} = \frac{21}{16} \int dt \frac{G m_1 m_2}{r} v_1^2 v_2^4 + \frac{3}{2} \int dt \frac{G^2 m_2^2 m_1}{r^2} v_1^2 \times \left[\frac{7}{2} v_2^2 + \frac{(\vec{v}_2 \cdot \hat{r})^2}{2} + \frac{1}{3}\frac{G m_2}{r} \right] + (1 \leftrightarrow 2), \tag{3.48}$$

and

[13] Index "r" stands for "renormalized," though in the current work we will not encounter divergences associated with nontrivial RG flow of the mass.

[14] We omit index "r" to avoid abuse of notation.

$$\text{Fig. 29(d)} = \frac{49}{64}\int dt \frac{Gm_1m_2}{r} v_1^4 v_2^4 + \frac{7}{8}\int dt \frac{G^2m_2^2m_1}{r^2} v_1^4\left[\frac{7}{2}v_2^2 + \frac{(\vec{v}_2\cdot\hat{r})^2}{2} + \frac{1}{3}\frac{Gm_2}{r}\right] + \frac{7}{8}\int dt \frac{G^2m_1^2m_2}{r^2} v_2^4\left[\frac{7}{2}v_1^2 + \frac{(\vec{v}_1\cdot\hat{r})^2}{2} + \frac{1}{3}\frac{Gm_1}{r}\right] + \frac{\pi^2}{64}\int dt \frac{G^3m_1^2m_2^2}{r^3}\left[(\vec{v}_1\cdot\vec{v}_2)^2 - \frac{59}{2}v_1^2v_2^2 + \frac{87}{2}v_1^2(\vec{v}_2\cdot\hat{r})^2 + \frac{87}{2}v_2^2(\vec{v}_1\cdot\hat{r})^2 + \frac{15}{2}(\vec{v}_2\cdot\hat{r})^2(\vec{v}_1\cdot\hat{r})^2 - 6(\vec{v}_2\cdot\hat{r})(\vec{v}_1\cdot\hat{r})(\vec{v}_1\cdot\vec{v}_2)\right] + \frac{1}{3}\int dt \frac{G^4m_1^2m_2^3}{r^4}\left[v_1^2\left(\frac{23}{2} - 8\gamma - 8\ln(r/L)\right) + (\vec{v}_1\cdot\hat{r})^2\left(-\frac{3}{2} + 2\gamma + 2\ln(r/L)\right)\right] + \frac{1}{3}\int dt \frac{G^4m_1^3m_2^2}{r^4}\left[v_2^2\left(\frac{23}{2} - 8\gamma - 8\ln(r/L)\right) + (\vec{v}_2\cdot\hat{r})^2\left(-\frac{3}{2} + 2\gamma + 2\ln(r/L)\right)\right] - \frac{4}{9}\int dt \frac{G^5m_1^3m_2^3}{r^5}[3 - 2\gamma - 2\ln(r/L)]. \tag{3.49}$$

To derive this expression we first applied (3.44) and then used transform Fourier master integrals of the appendix. Appearance of an arbitrary renormalization scale L in the above expression should not be taken as a strong evidence for a nontrivial RG flow, since if other terms in the full 4PN potential are considered then cancellation of logs might occur.

ACKNOWLEDGMENTS

It is a pleasure to thank Gabriele Veneziano for his lectures series "Transplanckian scattering" (Institute for Advanced Studies at Jerusalem, March 2009, based in part on [39,40]) which catalyzed the beginning of this work; Ofer Aharony, Ira Rothstein and Gerhard Schäfer for very useful comments on the manuscript; and finally the organizers of the following meetings where part of this work was performed: "The fifth Crete regional meeting in String Theory" (Crete, June–July 09), and "Gravity—New perspectives from strings and higher dimensions" (Benasque, July 09). In addition M. S. thanks the Perimeter Institute for their kind hospitality during the completion of this work. This research is supported by The Israel Science Foundation Grant no 607/05, by the German Israel Cooperation Project Grant DIP H.52, and the Einstein Center at the Hebrew University.

APPENDIX: MASTER INTEGRALS

In this appendix we present master integrals which we found useful during the calculations presented in the text. We start with

$$J = \int \frac{d^d\mathbf{q}}{(2\pi)^d}\frac{1}{(\mathbf{q}^2)^\alpha[(\mathbf{q}-\mathbf{k})^2]^\beta} = \frac{(\mathbf{k}^2)^{d/2-\alpha-\beta}}{(4\pi)^{d/2}}\frac{\Gamma(\alpha+\beta-d/2)}{\Gamma(\alpha)\Gamma(\beta)} \times \frac{\Gamma(d/2-\alpha)\Gamma(d/2-\beta)}{\Gamma(d-\alpha-\beta)} \tag{A1}$$

$$J_i = \int \frac{d^d\mathbf{q}}{(2\pi)^d}\frac{q_i}{(\mathbf{q}^2)^\alpha[(\mathbf{q}-\mathbf{k})^2]^\beta} = \frac{d/2-\alpha}{d-\alpha-\beta}Jk_i \tag{A2}$$

$$J_{ij} = \int \frac{d^d\mathbf{q}}{(2\pi)^d}\frac{q_iq_j}{(\mathbf{q}^2)^\alpha[(\mathbf{q}-\mathbf{k})^2]^\beta} = \frac{1}{(4\pi)^{d/2}}\frac{\Gamma(\alpha+\beta-d/2-1)}{\Gamma(\alpha)\Gamma(\beta)}\frac{\Gamma(d/2-\alpha+1)\Gamma(d/2-\beta)}{\Gamma(d-\alpha-\beta+2)} \times \left[(d/2-\alpha+1)(\alpha+\beta-d/2-1)k_ik_j + (d/2-\beta)\frac{\mathbf{k}^2}{2}\delta_{ij}\right](\mathbf{k}^2)^{d/2-\alpha-\beta} \tag{A3}$$

$$J_{ijk} = \int \frac{d^d\mathbf{q}}{(2\pi)^d}\frac{q_iq_jq_k}{(\mathbf{q}^2)^\alpha[(\mathbf{q}-\mathbf{k})^2]^\beta} = \frac{(\mathbf{k}^2)^{d/2-\alpha-\beta}}{(4\pi)^{d/2}}\frac{\Gamma(\alpha+\beta-d/2-1)}{\Gamma(\alpha)\Gamma(\beta)}\frac{\Gamma(d/2-\alpha+2)\Gamma(d/2-\beta)}{\Gamma(d-\alpha-\beta+3)} \times \left[(d/2-\alpha+2)(\alpha+\beta-d/2-1)k_ik_jk_k + (d/2-\beta)\frac{\mathbf{k}^2}{2}(\delta_{ij}k_k + \delta_{jk}k_i + \delta_{ik}k_j)\right] \tag{A4}$$

$$J_{ijkl} = \int \frac{d^d\mathbf{q}}{(2\pi)^d} \frac{q_i q_j q_k q_l}{(\mathbf{q}^2)^\alpha[(\mathbf{q}-\mathbf{k})^2]^\beta}$$
$$= \frac{(\mathbf{k}^2)^{d/2-\alpha-\beta}}{(4\pi)^{d/2}} \frac{\Gamma(d/2-\alpha+2)\Gamma(d/2-\beta)}{\Gamma(d-\alpha-\beta+4)} \frac{\Gamma(\alpha+\beta-d/2-2)}{\Gamma(\alpha)\Gamma(\beta)} \Big[(d/2-\beta)(d/2-\beta+1)(\delta_{ij}\delta_{kl}+\delta_{ik}\delta_{jl}+\delta_{il}\delta_{jk})$$
$$\times \frac{(\mathbf{k}^2)^2}{4} + (\delta_{ij}k_k k_l + \delta_{ik}k_j k_l + \delta_{il}k_j k_k + \delta_{jk}k_i k_l + \delta_{jl}k_i k_k + \delta_{kl}k_i k_j)\frac{\mathbf{k}^2}{2}(\alpha+\beta-d/2-2)(d/2-\alpha+2)$$
$$\times (d/2-\beta) + k_i k_j k_k k_l (\alpha+\beta-d/2-2)(\alpha+\beta-d/2-1)(d/2-\alpha+2)(d/2-\alpha+3)\Big]. \quad \text{(A5)}$$

As noticed in [9] the above integrals (A2)–(A5) of vector nature can be reduced to a scalar integral (A1) on the basis of their transformation properties under rotations. Yet such a reduction becomes involved when the rank of the tensor under consideration increases, and therefore we choose to list all those which were relevant to this work.

In order to evaluate the above integrals we proceed as follows. We first apply the generalized Feynman parametrization [38]

$$\prod_{i=1}^N \frac{1}{A_i^{m_i}} = \int_0^1 \prod_{i=1}^N dx_i \delta\Big(\sum x_i - 1\Big) \frac{\prod x_i^{m_i-1}}{[\sum x_i A_i]^{\sum m_i}} \times \frac{\Gamma(m_1+m_2+\cdots+m_N)}{\Gamma(m_1)\cdots\Gamma(m_N)} \quad \text{(A6)}$$

with $N=2$ and $m_1=\alpha$, $m_2=\beta$. Next we integrate over one of the Feynman parameters, e.g. x_2, and subsequently redefine the undetermined wave number $\mathbf{q} \to \mathbf{q} + x_1\mathbf{k}$.

Now, in order to integrate over $\mathbf{q}$, we build on the following formula

$$\int \frac{d^d\mathbf{q}}{(2\pi)^d} \frac{1}{(z\mathbf{q}^2+\Delta)^n} = \frac{z^{-d/2}}{(4\pi)^{d/2}} \frac{\Gamma(n-d/2)}{\Gamma(n)} \Delta^{d/2-n}, \quad \text{(A7)}$$

computed by means of dimensional regularization. Thus, for instance, differentiating it with respect to z a definite number of times and setting $z=1$, one obtains

$$\int \frac{d^d\mathbf{q}}{(2\pi)^d} \frac{\mathbf{q}^2}{(\mathbf{q}^2+\Delta)^n} = \frac{d/2}{(4\pi)^{d/2}} \frac{\Gamma(n-d/2-1)}{\Gamma(n)} \Delta^{d/2-n+1},$$
$$\int \frac{d^d\mathbf{q}}{(2\pi)^d} \frac{(\mathbf{q}^2)^2}{(\mathbf{q}^2+\Delta)^n} = \frac{d(d+2)}{4(4\pi)^{d/2}} \times \frac{\Gamma(n-d/2-2)}{\Gamma(n)} \Delta^{d/2-n+2}. \quad \text{(A8)}$$

As a final step we integrate over x_1.

Another set of useful identities is related to the following d-dimensional Fourier transform

$$\int \frac{d^d\mathbf{k}}{(2\pi)^d} \frac{e^{i\mathbf{k}\mathbf{r}}}{(\mathbf{k}^2)^\alpha} = \frac{1}{(4\pi)^{d/2}} \frac{\Gamma(d/2-\alpha)}{\Gamma(\alpha)} \Big(\frac{\mathbf{r}^2}{4}\Big)^{\alpha-d/2}. \quad \text{(A9)}$$

Differentiating it with respect to $\mathbf{r}$ yields

$$\int \frac{d^d\mathbf{k}}{(2\pi)^d} \frac{\mathbf{k}_i}{(\mathbf{k}^2)^\alpha} e^{i\mathbf{k}\mathbf{r}} = i x_i \frac{\Gamma(d/2-\alpha+1)}{2(4\pi)^{d/2}\Gamma(\alpha)} \Big(\frac{\mathbf{r}^2}{4}\Big)^{\alpha-d/2-1},$$
$$\int \frac{d^d\mathbf{k}}{(2\pi)^d} \frac{\mathbf{k}_i\mathbf{k}_j}{(\mathbf{k}^2)^\alpha} e^{i\mathbf{k}\mathbf{r}} = \frac{\Gamma(d/2-\alpha+1)}{(4\pi)^{d/2}\Gamma(\alpha)} \Big(\frac{\delta_{ij}}{2} + (\alpha-d/2-1) \times \frac{x_i x_j}{\mathbf{r}^2}\Big)\Big(\frac{\mathbf{r}^2}{4}\Big)^{\alpha-d/2-1} \quad \text{(A10)}$$

$$\int \frac{d^d\mathbf{k}}{(2\pi)^d} \frac{\mathbf{k}_i\mathbf{k}_j\mathbf{k}_l}{(\mathbf{k}^2)^\alpha} e^{i\mathbf{k}\mathbf{r}} = \frac{i\Gamma(d/2-\alpha+2)}{16(4\pi)^{d/2}\Gamma(\alpha)} \Big(\frac{\mathbf{r}^2}{4}\Big)^{\alpha-d/2-3} \times [\mathbf{r}^2(\delta_{il}x_j + \delta_{jl}x_i + \delta_{ij}x_l) - (d-2\alpha+4)x_i x_j x_l], \quad \text{(A11)}$$

$$\int \frac{d^d\mathbf{k}}{(2\pi)^d} \frac{\mathbf{k}_i\mathbf{k}_j\mathbf{k}_l\mathbf{k}_m}{(\mathbf{k}^2)^\alpha} e^{i\mathbf{k}\mathbf{r}}$$
$$= \frac{\Gamma(d/2-\alpha+3)}{32(4\pi)^{d/2}\Gamma(\alpha)} \Big(\frac{\mathbf{r}^2}{4}\Big)^{\alpha-d/2-4} \Big[(d-2\alpha+6)x_i x_j x_l x_m - \mathbf{r}^2(\delta_{im}x_j x_l + \delta_{jm}x_i x_l + \delta_{lm}x_i x_j + \delta_{il}x_m x_j + \delta_{jl}x_i x_m + \delta_{ij}x_l x_m) + \frac{(\mathbf{r}^2)^2}{(d-2\alpha+4)}(\delta_{il}\delta_{jm} + \delta_{jl}\delta_{im} + \delta_{ij}\delta_{lm})\Big]. \quad \text{(A12)}$$

[1] S. Rowan and J. Hough, Living Rev. Relativity **3**, 3 (2000); B. S. Sathyaprakash and B. F. Schutz, Living Rev. Relativity **12**, 2 (2009).
[2] F. Pretorius, arXiv:0710.1338.
[3] L. Blanchet, Living Rev. Relativity **5**, 3 (2002); Living Rev. Relativity **9**, 4 (2006); arXiv:0907.3596.
[4] G. Schaefer, arXiv:0910.2857.
[5] W. D. Goldberger and I. Z. Rothstein, Phys. Rev. D **73**, 104029 (2006); W. D. Goldberger, arXiv:hep-ph/0701129.
[6] H. Okamura, T. Ohta, T. Kimura, and K. Hiida, Prog. Theor. Phys. **50**, 2066 (1973).
[7] B. Kol and M. Smolkin, Phys. Rev. D **77**, 064033 (2008).
[8] B. Kol and M. Smolkin, Classical Quantum Gravity **25**, 145011 (2008).
[9] J. B. Gilmore and A. Ross, Phys. Rev. D **78**, 124021 (2008).
[10] W. D. Goldberger and I. Z. Rothstein, Phys. Rev. D **73**, 104030 (2006).
[11] B. Kol, Gen. Relativ. Gravit. **40**, 2061 (2008); Int. J. Mod. Phys. D **17**, 2617 (2008).
[12] T. Harmark, Phys. Rev. D **69**, 104015 (2004).
[13] D. Gorbonos and B. Kol, J. High Energy Phys. 06 (2004) 053.
[14] Y. Z. Chu, W. D. Goldberger, and I. Z. Rothstein, J. High Energy Phys. 03 (2006) 013.
[15] J. B. Gilmore, A. Ross, and M. Smolkin, J. High Energy Phys. 09 (2009) 104.
[16] R. A. Porto and I. Z. Rothstein, Phys. Rev. Lett. **97**, 021101 (2006).
[17] R. A. Porto, Phys. Rev. D **73**, 104031 (2006).
[18] M. Levi, arXiv:0802.1508.
[19] J. Steinhoff and G. Schafer, Europhys. Lett. **87**, 50 004 (2009).
[20] E. Barausse, E. Racine, and A. Buonanno, Phys. Rev. D **80**, 104025 (2009).
[21] T. Damour and A. Nagar, Phys. Rev. D **80**, 084035 (2009); T. Damour and O. M. Lecian, Phys. Rev. D **80**, 044017 (2009).
[22] T. Binnington and E. Poisson, Phys. Rev. D **80**, 084018 (2009).
[23] R. Emparan, T. Harmark, V. Niarchos, N. A. Obers, and M. J. Rodriguez, J. High Energy Phys. 10 (2007) 110.
[24] R. Emparan, T. Harmark, V. Niarchos, and N. A. Obers, arXiv:0910.1601.
[25] Y. Z. Chu, Phys. Rev. D **79**, 044031 (2009).
[26] M. Headrick, S. Kitchen, and T. Wiseman, arXiv:0905.1822.
[27] V. Cardoso, O. J. C. Dias, and P. Figueras, Phys. Rev. D **78**, 105010 (2008).
[28] C. R. Galley and M. Tiglio, Phys. Rev. D **79**, 124027 (2009).
[29] J. S. Schwinger, Proc. Natl. Acad. Sci. U.S.A. **37**, 452 (1951); **37**, 455 (1951); F. J. Dyson, Phys. Rev. **75**, 1736 (1949).
[30] K. Blagoev, F. Cooper, J. Dawson, and B. Mihaila, Phys. Rev. D **64**, 125003 (2001).
[31] M. Duetsch and K. Fredenhagen, Commun. Math. Phys. **243**, 275 (2003).
[32] T. Ledvinka, G. Schaefer, and J. Bicak, Phys. Rev. Lett. **100**, 251101 (2008).
[33] R. Alkofer and L. von Smekal, Phys. Rep. **353**, 281 (2001).
[34] T. Damour, P. Jaranowski, and G. Schaefer, Phys. Lett. B **513**, 147 (2001); L. Blanchet, T. Damour, and G. Esposito-Farese, Phys. Rev. D **69**, 124007 (2004); L. Blanchet, T. Damour, G. Esposito-Farese, and B. R. Iyer, Phys. Rev. D **71**, 124004 (2005).
[35] U. Cannella and R. Sturani, arXiv:0808.4034.
[36] J. D. Bjorken and S. S. Drell, *Relativistic Quantum Fields* (McGraw-Hill, New York, 1965), Chap. 19, p. 293.
[37] C. Itzykson and J.-B. Zuber, *Quantum Field Theory* (McGraw-Hill, New York, 1980), Chap. 10, p. 475.
[38] M. E. Peskin and D. V. Schroeder, *An Introduction To Quantum Field Theory* (Addison-Wesley, Reading, MA, 1995), p. 842.
[39] D. Amati, M. Ciafaloni, and G. Veneziano, Nucl. Phys. **B403**, 707 (1993).
[40] D. Amati, M. Ciafaloni, and G. Veneziano, J. High Energy Phys. 02 (2008) 049.